NASA/TM—2012–215978

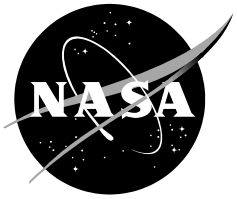

Flight Test Results on the Stability and Control of the F-15 Quiet Spike™ Aircraft

Cheng M. Moua, Shaun C. McWherter, and Timothy H. Cox

Dryden Flight Research Center, Edwards, California

Joe Gera, retired

Dryden Flight Research Center, Edwards, California

February 2012

NASA STI Program ... in Profile

Since its founding, NASA has been dedicated to the advancement of aeronautics and space science. The NASA scientific and technical information (STI) program plays a key part in helping NASA maintain this important role.

The NASA STI program operates under the auspices of the Agency Chief Information Officer. It collects, organizes, provides for archiving, and disseminates NASA's STI. The NASA STI program provides access to the NASA Aeronautics and Space Database and its public interface, the NASA Technical Report Server, thus providing one of the largest collections of aeronautical and space science STI in the world. Results are published in both non-NASA channels and by NASA in the NASA STI Report Series, which includes the following report types:

- TECHNICAL PUBLICATION. Reports of completed research or a major significant phase of research that present the results of NASA Programs and include extensive data or theoretical analysis. Includes compilations of significant scientific and technical data and information deemed to be of continuing reference value. NASA counterpart of peer-reviewed formal professional papers but has less stringent limitations on manuscript length and extent of graphic presentations.

- TECHNICAL MEMORANDUM. Scientific and technical findings that are preliminary or of specialized interest, e.g., quick release reports, working papers, and bibliographies that contain minimal annotation. Does not contain extensive analysis.

- CONTRACTOR REPORT. Scientific and technical findings by NASA-sponsored contractors and grantees.

- CONFERENCE PUBLICATION. Collected papers from scientific and technical conferences, symposia, seminars, or other meetings sponsored or co-sponsored by NASA.

- SPECIAL PUBLICATION. Scientific, technical, or historical information from NASA programs, projects, and missions, often concerned with subjects having substantial public interest.

- TECHNICAL TRANSLATION. English-language translations of foreign scientific and technical material pertinent to NASA's mission.

Specialized services also include organizing and publishing research results, distributing specialized research announcements and feeds, providing help desk and personal search support, and enabling data exchange services.

For more information about the NASA STI program, see the following:

- Access the NASA STI program home page at *http://www.sti.nasa.gov*

- E-mail your question via the Internet to help@sti.nasa.gov

- Fax your question to the NASA STI Help Desk at 443-757-5803

- Phone the NASA STI Help Desk at 443-757-5802

- Write to:
  NASA STI Help Desk
  NASA Center for AeroSpace Information
  7115 Standard Drive
  Hanover, MD 21076-1320

NASA/TM—2012–215978

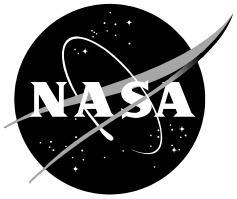

Flight Test Results on the Stability and Control of the F-15 Quiet Spike™ Aircraft

Cheng M. Moua, Shaun C. McWherter, and Timothy H. Cox

Dryden Flight Research Center, Edwards, California

Joe Gera, retired

Dryden Flight Research Center, Edwards, California

National Aeronautics and
Space Administration

Dryden Flight Research Center
Edwards, CA 93523-0273

February 2012

Available from:

NASA Center for AeroSpace Information
7115 Standard Drive
Hanover, MD 21076-1320
443-757-5802

Abstract

The Quiet Spike™ (Gulfstream Aerospace Corporation, Savannah, Georgia) F-15B (McDonnell Douglas Aerospace, now The Boeing Company, Chicago, Illinois) flight research program investigated supersonic shock reduction using a 24-ft sub-scale telescoping nose boom on an F-15B airplane. The primary flight-test objective was to collect flight data for aerodynamic and structural models validation up to Mach 1.8. Other objectives were to validate the mechanical feasibility of a morphing fuselage at the operational conditions and determine the near-field shock wave characterization. The stability and control objectives were to assess the effect of the spike on the stability, controllability, and handling qualities of the airplane and to ensure adequate stability margins across the entire research flight envelope. The two main stability and control challenges were that the effects of the telescoping nose boom influenced aerodynamics on the F-15B airplane flight dynamics and the air data and angle-of-attack sensors. This report discusses the stability and control flight envelope clearance methods and flight-test analysis of the F-15B Quiet Spike™. Brief pilot commentary on typical piloting tasks, approach and landing, the refueling task, and air data sensitivity to the flight control system are also described.

Nomenclature

accel	acceleration
alpha	angle of attack, deg
ANG	normal acceleration, g
ANY	lateral acceleration, g
beta	angle of sideslip, deg
CAP	control anticipation parameter, g^{-1}/s^{-2}
CAS	control augmentation system
$C_{D_{\alpha\beta}}$	airplane drag coefficient due to angle of attack and angle of sideslip, per deg
$C_{l_{da}}$	rolling moment coefficient due to aileron deflection, per deg
$C_{l_{dr}}$	rolling moment coefficient due to rudder deflection, per deg
$C_{l_{dt}}$	rolling moment coefficient due to differential stabilator deflection, per deg
C_{l_p}	rolling moment coefficient due to roll rate variation, per rad
C_{l_r}	rolling moment coefficient due to yaw rate variation, per rad
C_{l_β}	rolling moment coefficient due to sideslip variation, per deg
C_{L_α}	airplane lift coefficient due to angle of attack, per deg
$C_{m_{dh}}$	pitching moment coefficient due to symmetric stabilator deflection, per deg
C_{m_q}	pitching moment coefficient due to pitch rate variation, rad/s
C_{m_α}	pitching moment coefficient due to angle-of-attack variation, per deg
C_n	yawing moment coefficient
$C_{n_{da}}$	yawing moment coefficient due to aileron deflection, per deg
$C_{n_{dr}}$	yawing moment coefficient due to rudder deflection, per deg

$C_{n_{dt}}$	yawing moment coefficient due to differential stabilator deflection, per deg
C_{n_p}	yawing moment coefficient due to roll rate variation, per rad
C_{n_r}	yawing moment coefficient due to yaw rate variation, per rad
C_{n_β}	yawing moment coefficient due to sideslip variation, per deg
C_{Y_β}	side force coefficient due to sideslip, per deg
dad	differential aileron position, deg
dep	pitch stick deflection, in.
dhd	symmetric stabilator position, deg
dr	rudder position, deg
drd	symmetric rudder position, deg
dtd	differential stabilator deflection, deg
DFRC	Dryden Flight Research Center
FCS	flight control system
g	acceleration of gravity, ft/s^2
I_{XX}	airplane moment of inertia about the X-axis, slug-ft^2
I_{XZ}	airplane product of inertia about the XY axis, slug-ft^2
I_{YY}	airplane moment of inertia about the Y axis, slug-ft^2
I_{ZZ}	airplane moment of inertia about the Z axis, slug-ft^2
kft	represents 1,000 ft
KCAS	knots calibrated airspeed
MAC	mean aerodynamic chord
NASA	National Aeronautics and Space Administration
Ps	static pressure, lb/ft^2
Pt	total pressure, lb/ft^2
q	pitch rate, deg/s
Qbar	dynamic pressure, psf
qs	static pressure, psf
QS	Quiet Spike™
r	yaw rate, deg/s
sym	symmetric
SMI	structural mode interaction
xcg	center of gravity location in the X axis, % MAC

Introduction

This is a follow-on report that compliments NASA/TM-2009-214651, "Stability and Control Analysis of the F-15B Quiet Spike™ Aircraft." That report focuses primarily on pre-flight stability and control analysis; this report provides a brief overview of the pre-flight analysis and focuses primarily on the stability and control flight-test portion of the test project.

The Federal Aviation Administration restricts supersonic flight, except in special military flight corridors, to prevent aircraft from causing sonic booms over populated areas. This represents a significant obstacle for aircraft manufacturers who wish to produce supersonic civilian transport aircraft. Finding a way to suppress or "soften" the sonic boom of a supersonic aircraft could open the way to the production of a new generation of supersonic civilian aircraft.

The Quiet Spike™ is a technology concept developed by Gulfstream Aerospace Corporation (Savannah, Georgia) as a potential method for softening the sonic boom in smaller supersonic aircraft by partitioning the transonic shock wave into a series of smaller shock waves along a segmented boom extending from the front of an aircraft. Gulfstream approached the National Aeronautics and Space Administration (NASA) Dryden Flight Research Center (DFRC) (Edwards, California) as a research partner to conduct flight tests of the Quiet Spike™ on an existing F-15 airplane (McDonnell Douglas Aerospace, now The Boeing Company, Chicago, Illinois). Gulfstream provided a sub-scale Quiet Spike™, properly sized to mount on the radar bulkhead of an F-15 airplane, for NASA DFRC to install on the F-15B airplane. In addition to installation of the Quiet Spike™, NASA DFRC was responsible for conducting ground tests and flight tests, and for maintaining range safety. The Quiet Spike™ is referred to simply as "spike" within the body of this report.

The primary objectives of the flight research program were to verify the structural dynamics and loads of the spike up to Mach 1.8, validate the mechanical systems, and characterize the near-field shock waves produced by the spike. In the area of stability and control, the primary objectives were to assess the effect of the spike on the stability, controllability, and handling qualities of the F-15B airplane and to ensure adequate stability margins across the entire spike flight envelope. This report discusses the stability and control methods used for the flight envelope clearance and flight-test analysis of the F-15B spike configuration, primarily focusing on the spike-extended configuration. Brief pilot commentary on typical piloting tasks, approach and landing, the refueling task, and air data sensitivity to the flight control system are also discussed.

The Test Airplane

The test airplane is the two-seat version of the F-15 tactical fighter airplane built by the McDonnell Aircraft and Missile Systems division of the Boeing Company. Figure 1 shows the test airplane with the spike attached. The airplane has a data acquisition system with telemetry transmitters for ground monitoring and a research instrumentation system. A detailed description of the NASA DFRC F-15B airplane can be found in reference 1. Except for the installation of the sonic-boom suppressing spike, the only modification to the outer mold line of the production F-15B airplane was the addition of a sideslip vane to the underside just aft of the nose cone, and a fiberglass fairing over the gun port (refs. 2 and 3).

The Gulfstream Quiet Spike™

The spike is a telescopic nose boom that is mounted on the radar bulkhead of the F-15B test airplane and weighs approximately 450 lb. Additional details about the spike, along with dimensional data, are shown in figure 2. Information about the required modifications to the bulkhead internal forebody structure is contained in reference 4. As can be seen in figure 2, the length of the F-15B test airplane is increased by approximately 30 percent with the spike in the fully extended position, yet the changes to the mass and inertia characteristics are relatively modest. The mass and inertia characteristics are shown in table 1 for a mid-fuel loading of 8,000 lb.

Table 1. Mass and inertia characteristics of the baseline NASA Dryden Flight Research Center F-15B test airplane.

	Baseline F-15B test airplane	Spike retracted	Spike extended
Weight, lb	37,426	37,152	37,152
x_{cg}, % MAC	26.34	26.13	26.05
I_{XX}, slug-ft^2	30,345	27,947	27,953
I_{YY}, slug-ft^2	198,687	189,456	190,777
I_{ZZ}, slug-ft^2	223,214	212,746	213,957
I_{XZ}, slug-ft^2	-5,070	-466	-460

The control panel of the spike extension and retraction system was located in the aft cockpit of the F-15B test airplane. An electrically powered cable and pulley mechanism extended and retracted the spike (refs. 5-9).

The Flight Control System

The NASA DFRC F-15B control system consists of an integrated mechanical and electrical single-string, analog control augmentation system (CAS) operating in parallel to command the stabilators (deflected symmetrically for pitch and differentially for roll), ailerons, and rudders. Typical inceptors (stick and rudder pedals) are used for piloted control. The CAS is a single-string system in each of the three axes: pitch, roll, and yaw. Each axis can be engaged or disengaged in the cockpit. No changes were made to the production aircraft control system.

Mechanical pitch control is achieved mainly through a pitch ratio adjust device (PRAD). This mechanical device automatically adjusts the gain on the stick path based on static and total pressure to provide desirable stick force per acceleration of gravity (g). The only other feedback to the mechanical system is normal acceleration, which is used to trim the stabilator to a commanded g from the stick input. The pitch CAS (figure 3) provides closed-loop control of blended aircraft acceleration and pitch rate, commanding the equivalent of normal acceleration in up-and-away flight and providing Level 1 handling qualities (ref. 10). When the landing gear is down, the normal acceleration feedback is bypassed and the system provides pitch rate command. The pitch CAS also utilizes angle-of-attack feedback to induce a stall inhibitor when a certain angle of attack is reached.

The primary mechanical roll control system, shown in figure 4, contains the roll ratio adjust device (RRAD) and is augmented with a CAS. Similar to the PRAD, the RRAD varies the gain on the stick path based on the calibrated airspeed when the Mach number is greater than 1. The roll CAS provides closed-loop control of the aircraft roll rate. A roll CAS command limiter is scheduled with calibrated airspeed and angle of attack to reduce structural loads on the differential stabilator and provide compatible high-angle-of-attack differential stabilator control with the mechanical roll control system.

The mechanical yaw control system, shown in figure 5, illustrates the aileron-to-rudder interconnect (ARI), and the connection between the rudder pedal and the rudder. The ARI commands rudder deflections in response to lateral stick inputs, with the lateral stick-to-rudder

control surface deflections scheduled via the mechanical system symmetric stabilator. The ARI is only operative for Mach numbers below 1.0; otherwise, the ARI output is zero. The yaw CAS provides closed-loop control of blended aircraft lateral acceleration and yaw rate to augment Dutch roll damping and turn coordination. Roll coordination is achieved by a roll-to-yaw cross feed scheduled with angle of attack. The roll-to-yaw cross feed is nullified above Mach 1.5.

Description of the Simulation

The NASA DFRC simulation facility includes a dedicated fixed-base real-time pilot-in-the-loop F-15B simulator with standard stick and rudder pedal inceptors for pilot controls; head-up display; cockpit pilot flight instruments; and external real-time visual imagery. Oblate earth non-linear six-degrees-of freedom equations of motion are utilized. The simulation can be operated in a real-time, piloted mode or in a remote batch mode as an engineering analysis tool. Batch simulation runs may also be scripted to facilitate automated analysis (ref. 11).

To ensure a validated aerodynamic model, before installing the spike on the NASA DFRC F-15B test airplane, four research flights were conducted to gather data to validate and update the baseline aerodynamic model. Aerodynamic updates were implemented as increments to the baseline aerodynamic model in the simulation to improve overall time history comparisons between the simulation and flight data. These efforts validated the simulation as an analysis tool for the anticipated spike flight conditions and regimes. For a more detailed description of the aircraft baseline aerodynamic model and the updates see references 2 and 3.

Models of the Quiet Spike™

To ensure conservative estimates of the aerodynamic uncertainties, three independently developed aerodynamic models of the spike were implemented into the DFRC F-15B simulation for stability and control analysis (ref. 12). A model representing only the spike was developed by Gulfstream using an Euler computational fluid dynamics (CFD) method, which also incorporated empirical corrections. A second spike-only model was developed at DFRC using an aerodynamic vortex lattice modeling method for a subsonic model, flat plate theory, and empirical cone-cylinder drag data for a supersonic model. A third model was developed by Desktop Aeronautics Incorporated (DAI) (Palo Alto, California) using an Euler CFD method to model the full airplane as well as a full airplane-with-spike model. This final DAI spike model was extracted as a set of parameter deltas representing the difference between these two models. The differences between the three independently developed models were significant enough to motivate the inclusion of all three in the stability and handling qualities analysis. All three models were incorporated as additive delta values to the baseline F-15B aerodynamic model in the simulation. The deltas were applied to the following parameters: $C_{L_\alpha}, C_{D_\alpha}, C_{D_\beta}, C_{m_\alpha}, C_{n_\beta}, C_{y_\beta}$. Spike effects on the damping derivatives were not modeled and effects on the roll axis dynamics were estimated to be negligible. The effect of the spike on the airplane mass properties was also modeled; the spike did not significantly alter the center of gravity of the airplane. A build-up approach in flight-testing was followed to check the validity of these models as the flight envelope was expanded.

Pre-flight Simulation Analysis

The flight project utilized a build-up approach to minimize technical risk and ensure safety. Extensive simulation analysis was performed to evaluate the robustness of the F-15B Quiet Spike™ stability and flying qualities to aerodynamic uncertainties. These uncertainties

incorporated baseline F-15B aerodynamic model uncertainty, as well as spike aerodynamic uncertainty (ref. 3). The analysis was accomplished in an automated batch fashion using two DFRC-developed simulation software tools: a simulation run tool and a linear analysis tool. The analysis tool validated the linear models and calculated the parameters of stability and handling qualities based on the linear aerodynamic models and other models generated from the simulation run tool. The simulation test cases evaluated the nominal aerodynamics and aerodynamic stress cases for both CAS "on" and CAS "off;" three different fuel weights; and all three spike aerodynamic models with the spike fully extended, and to a limited degree, with the spike fully retracted.

The run tool generated response time history data and linear aerodynamic models for over 24,000 run cases for the combined subsonic, transonic, and supersonic analysis phases. The analysis tool evaluated all of the run cases that were generated by the run tool. Analysis cases that were flagged by the analysis tool for violation of handling qualities criteria were used to define critical flight conditions and configurations. The worst cases among those flagged were selected for further investigation by pilot-in-the-loop simulation exercises.

As a result of the stress analysis and pilot-in-the-loop simulation, regions of acceptable aerodynamic variations for key aerodynamic parameters were defined. Not only do these regions provide a measure of the robustness of the F-15B spike configuration, but they also provided guidance for the flight-test clearance approach. It should be noted that through lateral-directional analysis of the robust test cases, stability margins were inadequate for conditions from Mach 1.6 to Mach 1.8 when full aerodynamic uncertainties were applied. Aerodynamic uncertainties were reduced to three-fourths of their original values for analysis conditions higher than Mach 1.4 to ensure adequate stability margins for all analysis conditions for both the CAS-"on" and CAS-"off" configurations. The reduction of uncertainties during analysis was justified by imposing a markedly reduced tolerance for uncertainty in critical aerodynamic parameters during post-flight parameter estimation after each flight-test condition before clearing the next test condition in the flight envelope. More detailed information on the pre-flight simulation analysis can be found in reference 11.

Ground Tests

Ground vibration tests, ground loads calibration tests, structural mode interaction (SMI) tests, and taxi tests were conducted with the spike installed in preparation for flight (ref. 13). Three of the four ground tests indicated satisfactory results. Structural mode interaction tests, however, revealed lower-than-desired gain margins with the spike in the fully retracted configuration. The spike-retracted, gear-up configuration was identified as potentially susceptible to SMI limit cycle oscillations, indicating that the spike-extended configuration was more stable than the spike-retracted configuration (ref. 8). For this reason, flight envelope clearance was performed primarily in the spike-extended configuration.

Subsonic, Transonic, and Supersonic Flight Phases

The flight project was split into two phases, a subsonic phase and a supersonic phase, to allow the spike-equipped airplane to begin flight-testing while pre-flight analysis at the transonic and supersonic flight regimes was being performed. Splitting the project into two phases enabled an earlier checkout of the functionality of the mechanical system of the spike and of the operations of the spike under flight loads.

The subsonic phase was for all flight conditions up to and including Mach 0.8. A build-up approach progressing from low to high dynamic pressure and Mach number was used to clear the flight envelope. The majority of the flight envelope clearance was performed with the CAS "on" and a limited number with the CAS "off." Although batch simulation analysis results indicated no concerns with CAS-"off" dynamics for Mach numbers lower than 0.8, piloted simulation studies indicated poorer damping, which is especially undesirable in the yaw axis at higher dynamic pressure. The limited CAS-"off" flight conditions were flown to determine realism of the poor damping concerns, validate the simulation analysis tool with flight data, and provide confidence in the simulation results in the transonic and supersonic regions. To evaluate the CAS-"off" flight conditions, a range of acceptable time to half-amplitude, and period of the Dutch roll and short-period modes, were determined from the simulation stress analysis. These parameters plotted against dynamic pressure for three fuel weights formed a region where estimates from flight-testing would be expected to fall.

The transonic and supersonic phases were for flight conditions with Mach numbers higher than 0.8. Piloted simulation studies indicated that the CAS-"off" damping was highly oscillatory, which is especially undesirable in the transonic and supersonic regions. Only CAS-"on" conditions, therefore, were flown. In the event of an unanticipated reversion to a CAS-"off" condition while in flight, a procedure was established to maintain wings-level and decelerate to a safe region (slower than 250 kn). An additional constraint was placed on the pilot to minimize maneuvering during the deceleration. These restrictions were implemented as emergency procedures addendums.

Flight-testing above Mach 1.4 proceeded more cautiously. This cautionary requirement was in place because the stability and control simulation stress analysis required three-quarters aerodynamic uncertainties to ensure adequate stability. Flight conditions with Mach number increments no more than 0.05 were flown on a single flight, and post-flight data analysis was required to ensure adequate stability and handling qualities prior to proceeding to the higher Mach number condition.

The Limits of the Airplane with the Spike Installed

The flight envelope of the spike-equipped airplane was restricted to mitigate the hazards associated with the Quiet Spike™ experiment and reduce the number of flight-test conditions needed to meet project objectives. The angle of attack was restricted to 21 units (approximately 10.5 deg) for the clean configuration and 23 units (approximately 12 deg) for the landing configuration. Note that the angle-of-attack limits are established to avoid vortex shedding from the spike and to mitigate potential SMI problems that were identified during ground tests at higher angles of attack. The normal load factor for the NASA DFRC F-15B test airplane was limited between zero and three. The maximum dynamic pressure was limited to 685 lb/ft^2, and the maximum Mach number was limited to 1.8. Additionally, the maximum sink rate for landing was restricted to maximum 5 ft/s (300 ft/min). An additional flight dynamic limit, based on previous F-15B flight-test fixture design and flight-test experience, was a beta × Qbar (sideslip multiplied by dynamic pressure) of 5,500 deg psf. Additional maneuvering guidelines were placed on a beta × Qbar of 3000 deg psf. All stability and control testing was accomplished either in the fully extended or retracted positions. The time required for full extension or retraction is approximately 20 s.

Flight Envelope Clearance

Flight envelope clearance is a multi-step process that includes real-time assessment in the control room and post-flight simulation-to-flight-data comparisons. Using a build-up approach, test points were flown from low to high airspeed and dynamic pressure. Pitch, roll, and yaw doublets with small, medium, and large piloted stick inputs were the primary maneuvers for stability and control flight clearance. A well-damped airplane dynamic response to each doublet was the criterion for proceeding to the next maneuver. Post-flight, time history and aerodynamic derivations comparisons between flight and simulation were performed. Initial flight data, which included Mach number, altitude, airspeed, fuel weight, and flight data history data (which included piloted stick and rudder inputs or airplane surface positions for each maneuver) were input into the non-linear simulation for time history comparisons. Favorable comparisons of airplane dynamic responses were required to proceed to the next set of flight conditions. Although both the piloted inputs and airplane surface positions were used to drive the simulator for flight-to-simulator comparisons, only the piloted inputs are presented in this report. It should be noted, however, that flight-to-simulator comparisons with piloted inputs and airplane surface positions are similar. Three representative flight conditions, one each from the subsonic, transonic, and supersonic flight regime, were selected to show representative quality of the matches between flight and simulation. The three representative flight conditions are described in table 2.

Table 2. Representative flight conditions.

Representative flight condition	Altitude, kft	Mach number
1	25	.60
2	35	.95
3	45	1.80

In addition to comparing airplane responses between flight and simulation, post-flight estimates of the aerodynamic derivatives were also compared to the regions of acceptable aerodynamic variations that had been determined during the pre-flight simulation analysis. The aerodynamic derivatives of interest included: C_{m_α}, $C_{m_{dh}}$, and C_{m_q} in the pitch axis; C_{l_β}, $C_{l_{dr}}$, $C_{l_{da}}$, $C_{l_{dt}}$, C_{l_p}, and C_{l_r} in the roll axis; and C_{n_β}, C_{n_r}, $C_{n_{dr}}$, $C_{n_{da}}$, $C_{n_{dt}}$, C_{n_p}, and C_{Y_β} in the yaw axis. If the flight-estimated stability derivative trends observed as a function of Mach number projected that subsequent Mach number expansion points fell within the predicted regions, then the F-15B spike would be cleared to perform flight envelope expansion at those points. If the projected trends indicated that an aerodynamic derivative fell outside its region, then further analysis would be warranted before expanding the flight envelope.

Flight-Test Results

A total of 30 flights were flown from August 10, 2006 to February 9, 2007 in support of the Quiet Spike™ flight project. Figure 6 shows the flight conditions flown in support of the project. The spike flew successfully through the subsonic, transonic, and supersonic flight regime up to Mach 1.8 in the extended configuration with the CAS “on.” Each flight condition in the subsonic

flight regime was successfully cleared with the CAS "off" prior to proceeding with the CAS "on." The airplane flew with the spike in the retracted configuration with the CAS "on" in the subsonic and transonic flight regime. The NASA DFRC F-15B test airplane with the attached spike was stable and controllable throughout the flight envelope as predicted by the extensive simulation analyses.

Since the effect of the spike on the roll responses is negligible, the flight-test results presented in this report focus on the pitch and yaw axis only. In addition, only the results with the spike in the extended configuration are presented, since the retracted configuration is generally the same or better. It should be noted that although ground-test analysis predicted SMI problems in the retracted configuration, no SMI problems were observed in flight.

Flight-to-Simulation Comparisons

The F-15B simulator agreed well with the flight data throughout the entire research flight envelope. Generally, excellent matches in airplane dynamic responses were achieved in the pitch and yaw axis for all flight conditions. Three representative simulator-to-flight comparisons are shown in figures 7-12. Pitch rate, alpha, normal acceleration, symmetric stabilator position, yaw rate, beta, and lateral acceleration between flight and simulation overlay each other. There was an observed phase difference, however, in the symmetric stabilator between flight and the simulator. The symmetric stabilator in the simulator was leading the flight by approximately 60 ms. The 60-ms delay was applied to the simulation symmetric stabilator and the pre-flight stress analysis was performed to verify the stability margins. A simulation comparison plot with and without the 60-ms delay is shown in figure 13. As seen in that figure, the pitch rate matches better with the time delay, and the time delay is observed to be conservative. With the time delay, the gain margin and phase margin were reduced at most by 7 dB and 25 deg, respectively, but still provided ample stability margins, as shown in figure 14. These favorable comparisons between flight and simulation made it easy to safely proceed to the next point at a higher dynamic pressure or Mach number.

Stability and Control Derivative Borders

In addition to flight-data-to-simulator time history comparisons, post-flight aerodynamic parameter estimation was used to assess the stability and controllability of the NASA DFRC F-15B test airplane with the spike attached. Most of the parameters estimated from flight data were well within the boundary of acceptable aerodynamic variations for both the subsonic and the supersonic flight regime. The parameters that showed the most variation from the nominal F-15B aerodynamic model values in the subsonic flight regime were C_{m_q}, C_{n_r}, and C_{n_β}; as shown in figures 15-17. For the subsonic flight envelope, C_{m_q} and C_{n_r} indicated less damping than the nominal F-15B aerodynamic model, as shown in figure 15 and figure 16, respectively. The data for C_{m_q} stayed at the border of the acceptable variations or slightly beyond it. Despite this, significant damping still existed in this parameter. For C_{n_r} the variations stayed within the previously defined acceptable regions. Estimated C_{n_β} in the subsonic regime also stayed well within the bounds, despite the large scatter at low speed.

The damping derivative C_{m_q} deviated outside the boundary at some transonic and supersonic conditions (less than at subsonic conditions). The first of these conditions of interest is observed in figure 18. At that point, data had been collected up to Mach 1.2 at an altitude of 45,000 ft. The

next series of flights was to expand the flight envelope to Mach 1.4. The trend in the data from Mach 1.2, extrapolated to Mach 1.4 in figure 18, indicated that C_{m_q} could fall outside the acceptable region based on the simulation stress analysis. This C_{m_q} trend, indicated by the dashed line, which shows an increase in damping from Mach 1.1 to Mach 1.2, did not follow the nominal F-15B aerodynamic model trend. Although the projected trend was not considered likely, the simulation was updated for the projected C_{m_q} at Mach 1.4 as a worst-case scenario, and the stability margins were recalculated. A piloted simulation evaluation of CAS-"off" dynamics is shown in figure 19. The pilot initiated a 2-g turn, turned the CAS "off," and then rolled out to initiate a wings-level deceleration to 250 kn, as called for by CAS-"off" procedure. The lightly-damped response, a damping ratio of approximately 0.03, was determined by the pilot to be undesirable but controllable for this task. Flight-testing proceeded to Mach 1.4, and the undesired projected trend in C_{m_q} was not observed. Figure 20 shows the flight-estimated C_{m_q} remaining at approximately the Mach 1.2 level of stability, and within the acceptable region, up to approximately Mach 1.7. At that point, a destabilizing trend is observed. Projecting this trend, observed in figure 20, to Mach 1.8 and repeating the analysis that was performed at Mach 1.4 showed again that stability was acceptable, and that CAS-"off" dynamics, although undesirable, were controllable. The same trend was observed in the flight data. Fortunately, the goal of the project was achieved at Mach 1.8, in spite of the fact that little margin was left for Mach expansion due to the C_{m_q}.

Estimated static stability derivatives, C_{m_α} and C_{n_β}, showed reasonable variations with respect to their boundaries. A rapid reduction in C_{n_β} occurred in the Mach 1.2 to Mach 1.4 regions, as shown in figure 21. When extrapolated to the next series of expansion points, C_{n_β} deviated to the lower boundary at Mach 1.4. Flight-testing continued cautiously but estimated C_{n_β} flattened out at the higher Mach numbers following the aerodynamic model trend and the limited baseline flight data at those conditions. The data for C_{m_α} were generally within the boundaries, as shown in figure 22. At Mach 1.1, C_{m_α} deviated slightly outside the upper boundary. Since C_{m_α} was still in the stable region, flight-testing proceeded. At Mach 1.2 C_{m_α} came back inside the boundaries and remained within the boundaries until Mach 1.8.

The C_{n_r} indicated less damping than the nominal F-15B aerodynamic model throughout the transonic and supersonic conditions, as shown in figure 23. Between Mach 1.5 and Mach 1.6, C_{n_r} deviated slightly outside the upper boundary. The projected trend for Mach 1.7 and Mach 1.8 conditions indicated that C_{n_r} would be slightly outside the upper boundary. Although flight-testing proceeded cautiously at these two flight conditions, C_{n_r} did not follow the projected trend. Instead, C_{n_r} stayed within the boundaries.

The Effect of the Spike on Airplane Dynamics with the Control Augmentation System "On" or "Off"

Prior to the flight-testing of the Quiet Spike™ project the piloted stick and pedal deflections were not instrumented on the baseline F-15B airplane. Therefore, data from the baseline F-15B flights were not suitable for comparison with the data from the spike-equipped airplane flights. Consequently, the effects of the spike on the dynamics of the baseline F-15B airplane were performed entirely with the simulator. It should be noted, however, that the F-15B simulator has been validated against the spike-equipped airplane throughout the research flight envelope and that the comparisons were excellent. Simulation comparisons between the spike-equipped airplane and the baseline F-15B test airplane were made at the three representative subsonic, transonic, and supersonic flight conditions described in table 2 above. Identical pitch and rudder pedal doublets were chosen for inputs to excite the spike-equipped and the baseline airplane simulations.

Selected CAS-"on" and CAS-"off" comparisons between the responses of the simulated spike-equipped test airplane and the simulated basic F-15B airplane are shown in figures 24-29. With the CAS "on," the effect of the spike on the pitch and yaw responses is very small. This is attributed to the relatively small aerodynamic effect of the spike on the overall aerodynamic characteristics of the F-15B airplane, negligible changes in the location of the center of gravity and moment of inertia characteristics, and the robustness of the CAS in the flight control system. With the CAS "off," there were some effects of the spike in the pitch and yaw axis airplane responses. The damping in the pitch axis was slightly less in the subsonic regime, more in the transonic regime, and much less in the supersonic regime. At Mach 1.8 the responses of the airplane were oscillatory from a pitch doublet and the magnitudes were increased with the spike. In the yaw axis the dampings were reduced for all three conditions with the spike. At Mach 0.95 more oscillations were observed.

Handling Qualities

Since handling qualities research was not a goal, no formal handling qualities evaluation was conducted during the flight tests. Brief pilot commentaries were collected, however, for typical piloting tasks, approach and landing, and the refueling task. Simple piloting tasks such as climbing, descending, and capturing and maintaining a flight condition, were conducted with the CAS in both the "on" and the "off" position in the subsonic regime (less than Mach 0.8); and with the CAS "on" in the transonic and supersonic regimes. Aerial refueling maneuvers were also used.

The flight results on the CAS-"off" clearance points with spike-extended conditions in the subsonic flight regime are shown in figures 30-33. The Dutch roll, Dutch roll time to half, the short period, and the short-period to half modes all fell within the expected stress analysis regions for the light, medium, and heavy fuel weights. The favorable results provided high confidence in the stability and controls simulation tools for the spike-attached F-15B airplane with the CAS "off."

Handling qualities were evaluated at an altitude of 20,000 ft and an airspeed of 275 KCAS to clear the F-15B test airplane with the attached spike for aerial refueling maneuvers with a KC-135 Stratotanker (The Boeing Company, Chicago, Illinois) refueling airplane. The handling qualities evaluation was performed with the F-15B test airplane in the spike fully-extended configuration to not only demonstrate the worst case condition with minimum calculated clearance distance between the two aircraft, but also because of concerns relative to SMI. A series

of tracking tasks were conducted with the F-15B test airplane at increasingly closer relative positions to the refueling airplane. The task involved the F-15B pilot tracking the refueling boom with a fixed reference point while the boom translated in a box pattern at various angles. Final clearance involved plugging the boom into the F-15B test airplane for actual refueling. During the clearance process, a chase airplane was required to verify adequate clearance between the spike tip and the refueling airplane. Aerial refueling clearance permitted increased flight efficiency by allowing multiple supersonic test points with minimal test flights. Aerial refueling of the fully-extended spiked F-15B airplane was similar to refueling a standard F-15B airplane. Post-flight analysis of photographs showed approximately 18 ft of horizontal clearance between the tip of the spiked F-15B airplane and the KC-135 airplane in the nominal contact position. Successful aerial refueling was performed with no deficiencies noted.

Pilot commentary indicated that the F-15B airplane with the attached spike handled similarly to a baseline F-15B airplane for all tasks in all flight phases. The CAS-"off" handling qualities in the subsonic regime (less than Mach 0.8) were adequate for typical piloting tasks. In supersonic flight, at approximately Mach 1.8, the pilot indicated a bit more "looseness" in the directional axis compared to the standard F-15B airplane, but he did not feel this was a significant handling qualities deficiency. Although the comparisons of rudder doublets of the simulation with and without the spike in figures 24-26 show very little deviation with the CAS "on," the CAS-"off" comparisons in figures 27-29 show small, relatively mild reductions in damping due to the spike. Figure 34 shows Dutch roll frequency and damping estimates for the three flight conditions described in table 2 above, generated with a linear model updated with parameter estimate data for the spike in the extended configuration, against Military Standard criteria (ref. 10). The small reductions in Dutch roll damping due to the spike are not significant enough to cross into the Level 2 region.

A CAS-"off," pitch axis handling qualities comparison of the baseline F-15B airplane and the F-15B airplane with the spike configuration was made using the simulation without the spike, and the simulation with the aerodynamics updated from parameter estimation. Frequency sweeps were inserted into the simulation and a low-order equivalent system fitting of the resulting frequency response provided estimates of the control anticipation parameter (CAP) and short-period damping. Analysis for the extended spike was conducted at the three flight conditions described in table 2 above to compare the spike effects and is summarized in figure 35. Generally, the short-period damping has been modified while the CAP remains relatively unaffected. For the 25,000-ft altitude and Mach 0.6 point, the reduction is within the Level 2 region and is not significant. This corresponds to the adequate CAS-"off" handling qualities indicated by flight experience. The short-period damping increases in the transonic region, which is consistent with parameter estimation where C_{m_q} becomes more negative than the baseline airplane at Mach 0.95, as seen in figure 20. At Mach 1.8, however, where the damping is quite low for the baseline airplane, the spike contributes an approximately 33-percent reduction to the short-period damping. This level of reduction in damping was determined in piloted simulation to be marginally acceptable for a level deceleration task, which was added as an addendum to emergency procedures for a CAS-"off" event.

The approach and landing task was conducted with the spike extended and the spike retracted. Toward the end of the project a series of touch-and-go and landings with increased sink rates at touchdown were performed for the purpose of documenting the spike loads. The piloting task was to target a -0.5 to -1.0 deg flight path at the moment the main wheels impacted the runway. To achieve the objective, the pilot positioned the flight path marker on the head-up

display relative to the pitch ladder. The display for this task, however, was not optimal due to the lack of resolution of the pitch ladder, which made it difficult to control the flight path precisely.

The ease and ability of controlling the flight path on approach and landing was validated with pilot comments as well. Figure 36 shows the estimated sink rates at touchdown across 12 touch-and-go's or landings compared to a targeted range, corresponding to -0.5 to -1.0 deg of flight path, identified for the objective of collecting loads data on the spike. Most of the estimated sink rates fall within the desired range, or within a few tenths ft/s. The largest deviation observed was 0.5 ft/s. Considering the display available to the pilot for controlling sink rate, this value verified the ability of the pilot to maintain a desired flight path.

Elevated Sideslip Angle Test Points

Due to the unanticipated low lateral loads measured in flight from the spike, higher lateral loading test points were added to the flight-test project; the elevated sideslip angle test points are described in table 3. Previously, the F-15B spike had been cleared within 6 deg of sideslip; additional higher beta sweeps and higher wings-level beta were planned to 12 deg true. The pilot's situational awareness was impaired as sideslip increased to higher levels; therefore, a control room display was required to alleviate concerns that a destabilizing non-linear yawing moment might develop as sideslip increased during the sweeps.

Table 3. Elevated sideslip angle test points.

Maneuver type	Altitude, kft	Mach number
Beta wings-level and beta sweeps	15	0.6
Beta wings-level and beta sweeps	15	0.8
Beta wings-level and beta sweeps	25	0.6
Beta wings-level and beta sweeps	35	0.6
Beta wings-level and beta sweeps	35	0.8
Loaded beta doublets	15	0.4
Loaded beta doublets	25	0.6
Loaded beta doublets	35	0.8

To aid in the development of a display, the simulation was updated with the addition of a term to artificially induce a non-linear yawing moment. Figure 37 shows the artificial yawing moment that was added and the total non-linear yawing moment that resulted for one flight condition. Notice that in the region between 7 and 8 deg the slope of C_n versus sideslip flattens and becomes zero. A display indicating this region where the yawing moment is becoming neutrally stable is necessary to avert an impending departure. Figure 38 shows a plot with simulation data of sideslip versus rudder position during a wings-level sideslip maneuver. At approximately 7 to 8 deg of sideslip a deviation from the linear region is noted. As a result, a real-time display of rudder position versus beta cross plot was implemented in the control room. With this display, wings-level sideslip maneuvers could be aborted when sideslip excursions occurred for relatively small rudder deflections.

Elevated sideslip angle flight-testing was completed up to 8 deg true beta. The initial plan was to test up to 12 deg, but the F-15B airplane with the spike attached did not allow for accurate beta calibration, which prevented testing beyond 8 deg. The beta maneuvers described in table 3 were flown in the subsonic flight regime in the spike fully extended and spike retracted configurations. Despite limited flight-testing, the flight-test approach using the cross plot of rudder position versus beta angle proved useful to alert the test team in avoiding potential sudden airplane departure. At one condition, shown in figure 39, the sideslip angle continued to increase while the rudder position remained relatively constant at approximately 8 deg. Using the flight parameters of lateral acceleration, ANY, and yaw rate, r, an estimated beta was computed; the estimated beta did not follow the same trend but was linear. To investigate whether this trend was due to sideslip calibration instead of a destabilizing non-linear yawing moment, yaw-roll doublets were performed at a series of constant betas with the spike in the extended configuration. The results are plotted in figure 40 as a function of the absolute value of sideslip. The C_{n_β} estimate appears to be linear from 0 to 5 deg beta. Although both the estimated beta calculation and the doublets performed at a constant beta suggested a sideslip angle calibration concern, had this been a true destabilizing non-linear yawing moment such would have been recognized in the control room and instruction would have been relayed to the pilot to abort the maneuver, to potentially avoid airplane departure.

Air Data Sensitivity

The flight control system in the pitch axis uses static and total pressures to set the stick gain. The spike could potentially change the airflow at the air data probes and modify the stick gain from the baseline value at a given condition. If this modification were significant, it could conceivably lead to a pilot-induced oscillation tendency or degraded handling qualities. The effects of the spike on the control system were evaluated using the pitch ratio gauge. This gauge, located in the cockpit, reflected the gain on the stick based on equation (1):

$$\text{Pitch ratio} = 0.2 * (\text{“stick gain”} / 0.6464 - 1) \quad (1)$$

For each new flight condition the pilot read the pitch ratio gauge to the research engineer sited in the control room to compare to the predicted values based on the contour lines of the pitch ratio; see figure 41. The new flight condition was cleared for flight-testing only after a good match was verified.

The pitch ratio gauge data was generally insensitive to the spike-induced changes to air data measurements throughout most of the flight envelope. Figure 42 shows a cross cut of the expected pitch ratio gauge at an altitude of 25,000 ft as a function of Mach number. The dashed lines shown in the figure encompass the tolerances in the mechanical system. Except at the Mach 1.05 condition, the gauge data read from the cockpit during flights fall within 0.1 of the anticipated value, and well within the tolerance levels. Time history comparisons of flight and simulation data at the 25,000-ft altitude and Mach 1.05 condition indicated the simulation overpredicts the magnitude of the response from the test doublets by 15 to 20 percent. Although this does not match the approximately 50-percent increase in magnitude predicted from the data shown in figure 42, it does indicate the spike has a small influence on the air-data-driven stick gain in the Mach 1.05 transonic region.

Conclusions

Flight-testing of the F-15B (McDonnell Douglas, now The Boeing Company, Chicago, Illinois) Quiet Spike™ (Gulfstream Aerospace Corporation, Savannah, Georgia) project was successfully completed in February 2007. The stability and control objectives, which were to assess the potentially destabilizing effect of the Quiet Spike™ on the stability, controllability, and handling qualities of the F-15B airplane and to ensure adequate stability margins, were met. The Quiet Spike™ flight envelope was cleared without incident in the fully-extended and the retracted configuration. The generally excellent dynamic response matches between flight and simulation provided high confidence in the simulation analysis tool and made it easy to proceed throughout the entire flight envelope. Post-flight parameter estimation of the aerodynamic derivatives provided trends that indicated possible deviation outside the acceptable aerodynamic variations for additional simulation analysis. Validating the simulator with flight data and then using the simulator to predict and ensure stability margins and handling qualities before flight-testing the next test conditions limited the risks to the test project.

The effect of the spike on the stability and control with the control augmentation system "on" was negligible; with the control augmentation "off," the control anticipation parameter remained relatively unaffected from the nominal F-15B aerodynamic model, while short-period damping was slightly modified. The short-period damping was unaffected in the subsonic region, increased in the transonic regime, and decreased in the supersonic region. Although the short-period damping was slightly affected, it still remained within the same Military Standard level.

Pilot commentary indicated that the spike-equipped F-15B airplane handled similarly to a standard F-15B airplane for all tasks in all flight phases. Successful refueling was performed with the spike extended with no deficiencies noted. The ease and ability of controlling the flight path on approach and landing was validated in pilot comments as well. The pitch ratio gauge data was generally insensitive to the spike-induced air data measurements throughout most of the flight envelope.

References

1. Richwine, David M., *F-15B/Flight Test Fixture II: A Test Bed for Flight Research*, NASA TM 4782, 1996.

2. Smolka, James W., Robert A. Cowart, Leslie M. Molzahn, Thomas J. Grindle, Tim Cox, and Steve Cumming et al., "Flight Testing of the Gulfstream Quiet Spike™ on a NASA F-15B," *Proceedings of the Society of Experimental Test Pilots 51st Symposium and Banquet*, Anaheim, California, September 26-29, 2007.

3. Cumming, Stephen B., Mark S. Smith, and Michael A. Frederick, "Aerodynamic Effects of an Oversized, Multi-Segmented Nose Boom on an F-15B," AIAA-2007-6638, August 2007.

4. Freund, Donald, Frank Simmons III, Natalie D. Spivey, and Lawrence Schuster, "Quiet Spike™ Prototype Flight Test Results," AIAA-2007-1778, April 2007.

5. Henne, Preston A., Donald C. Howe, Robert R. Wolz, and Jimmy L. Hancock Jr., "Supersonic Aircraft with Spike for Controlling and Reducing Sonic Boom," U.S. Patent Number 6698684, issued March 2, 2004.

6. Howe, Donald C., "Improved Sonic Boom Minimization with Extendable Nose Spike," AIAA-2005-1014, January 2005.

7. Howe, Donald C., "Sonic Boom Reduction Through the Use of Non-Axsymmetric Configuration Shaping," AIAA-2003-929, January 2003.

8. Simmons III, Frank, and Donald Freund, "Morphing Concept for Quiet Supersonic Jet Boom Mitigation," AIAA-2005-1015, January 2005.

9. Simmons III, Frank, Donald Freund, Natalie D. Spivey, and Lawrence Schuster, "Quiet Spike™: The Design and Validation of an Extendable Nose Boom Prototype," AIAA-2007-1774, April 2007.

10. U.S. Department of Defense, *Flying Qualities of Piloted Vehicles*, MIL-STD-1797, March 31, 1987.

11. McWherter, Shaun C., Cheng M. Moua, Joseph Gera, and Tim Cox, *Stability and Control Analysis of the F15-B Quiet Spike™ Aircraft,* NASA/TM-2009-214651, 2009.

12. Norlin, Ken A., *Flight Simulation Software at NASA Dryden Flight Research Center*, NASA TM-104315, 1995.

13. Spivey, Natalie D., Claudia Y. Herrera, Roger Truax, Chan-gi Pak, and Donald Freund, "Quiet Spike™ Build-up Ground Vibration Testing Approach," AIAA-2007-1175, April 2007.

Additional References

Haering Jr., Edward A., James E. Murray, Dana D. Purifoy, David H. Graham, Keith B. Meredith, and Christopher E. Ashburn, et al., "Airborne Shaped Sonic Boom Demonstration Pressure Measurements with Computational Fluid Dynamics Comparisons," AIAA-2005-9, January 2005.

Herrera, Claudia. Y., and Chan-gi Pak, "Build-up Approach to Updating the Mock Quiet Spike™ Beam Model," AIAA-2007-1776, April 2007.

Figures

ED06-0187-18

Figure 1. The NASA Dryden Flight Research Center F-15B testbed airplane with the Quiet Spike™ nose boom attached.

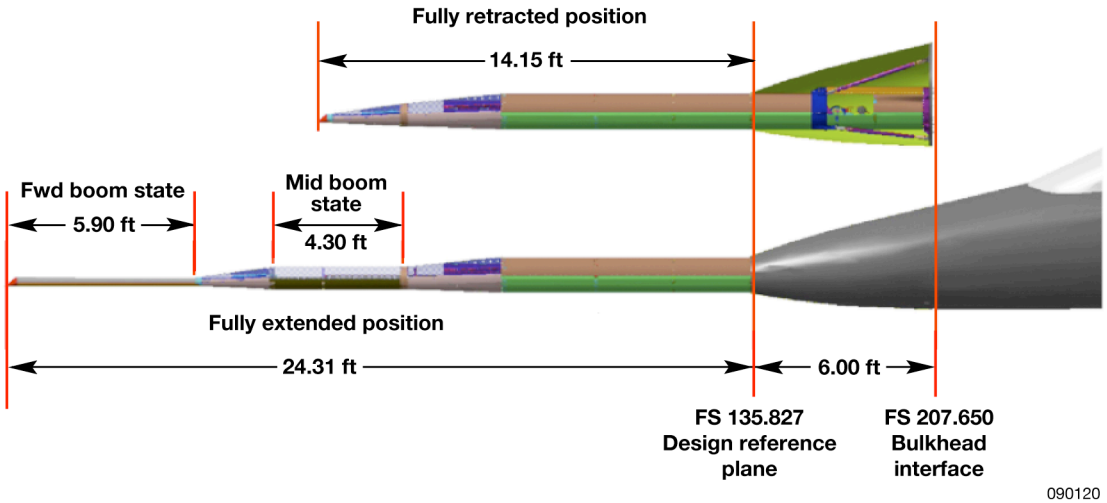

Figure 2. The Quiet Spike™ boom configuration.

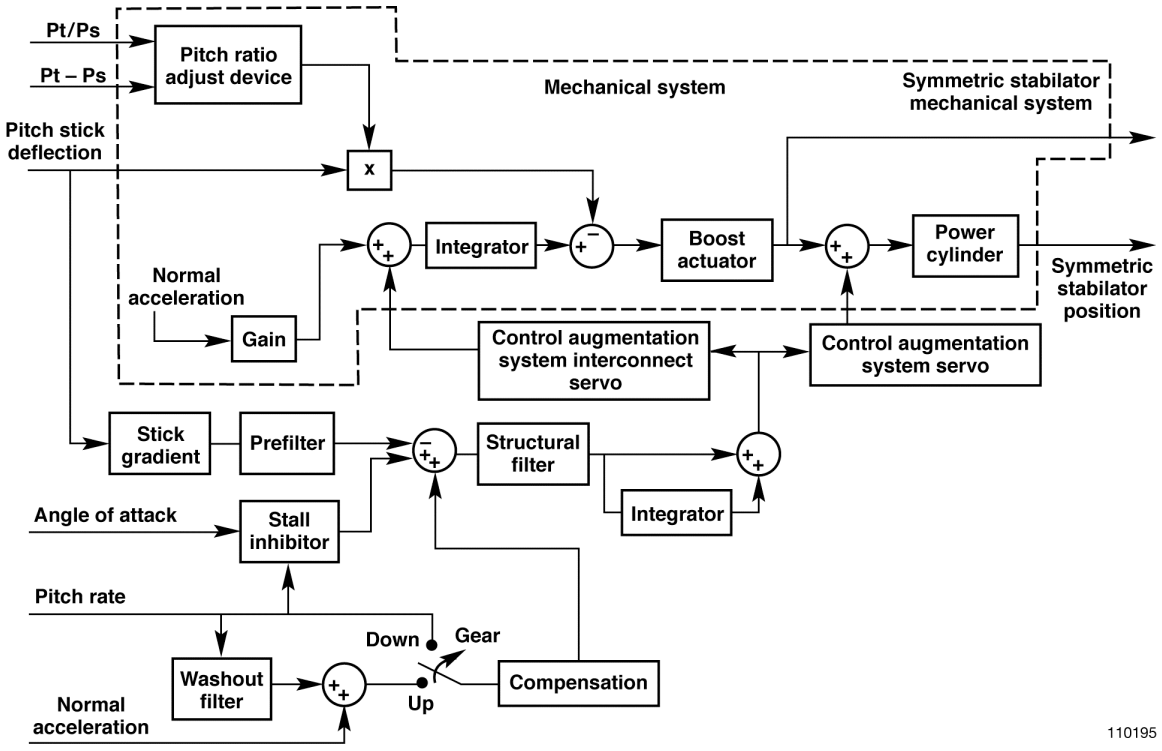

Figure 3. A simplified pitch axis control model for the NASA Dryden Flight Research Center F-15B test airplane.

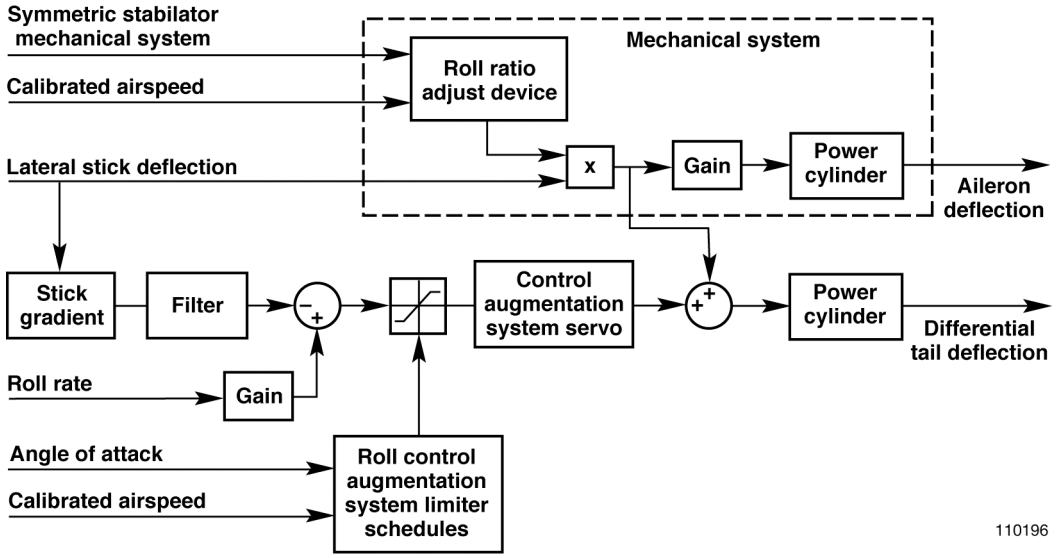

Figure 4. A simplified roll axis control model for the NASA Dryden Flight Research Center F-15B test airplane.

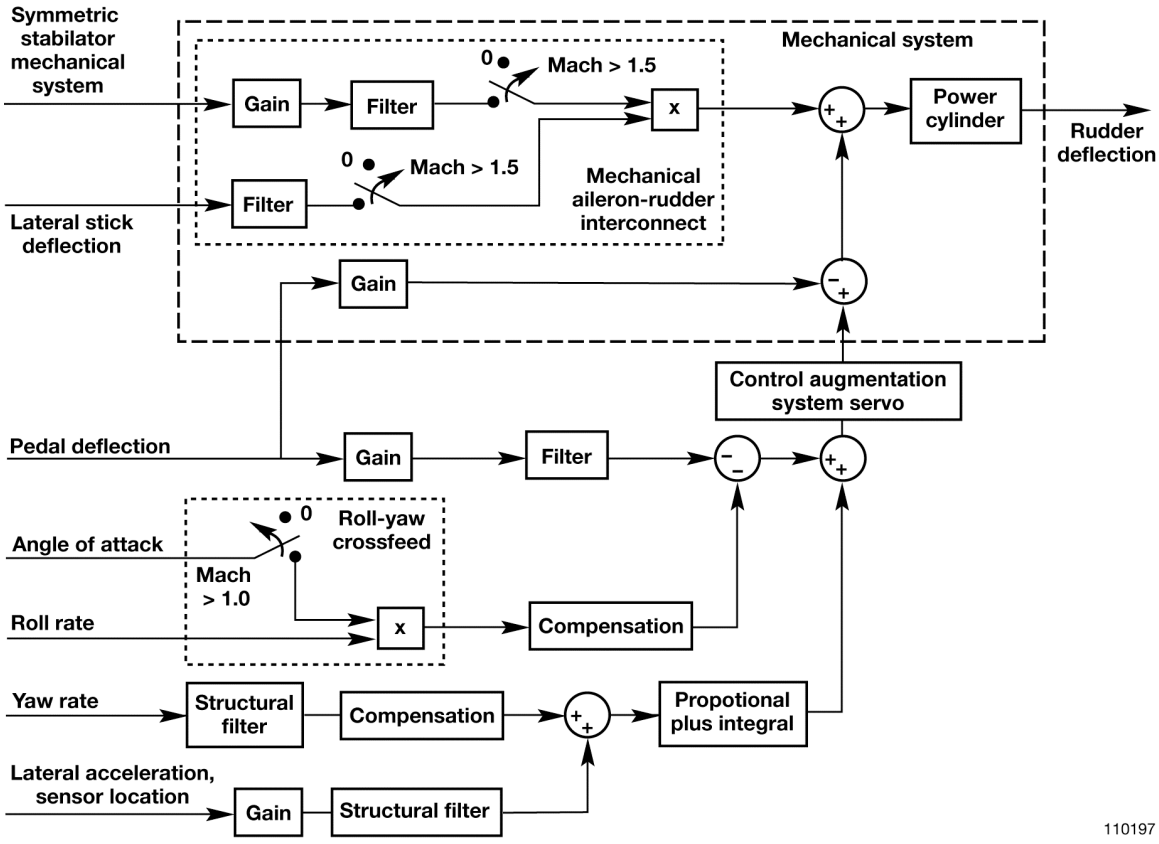

Figure 5. A simplified yaw axis control model for the NASA Dryden Flight Research Center F-15B test airplane.

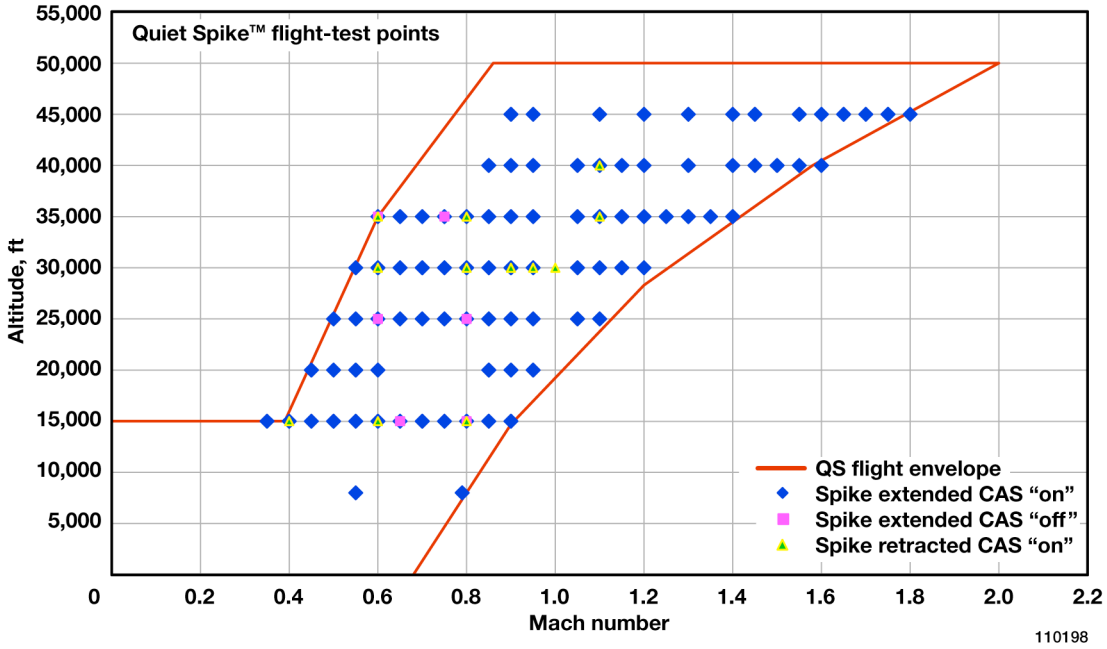

Figure 6. Quiet Spike™ flight-test points.

Figure 7. Subsonic pitch doublets.

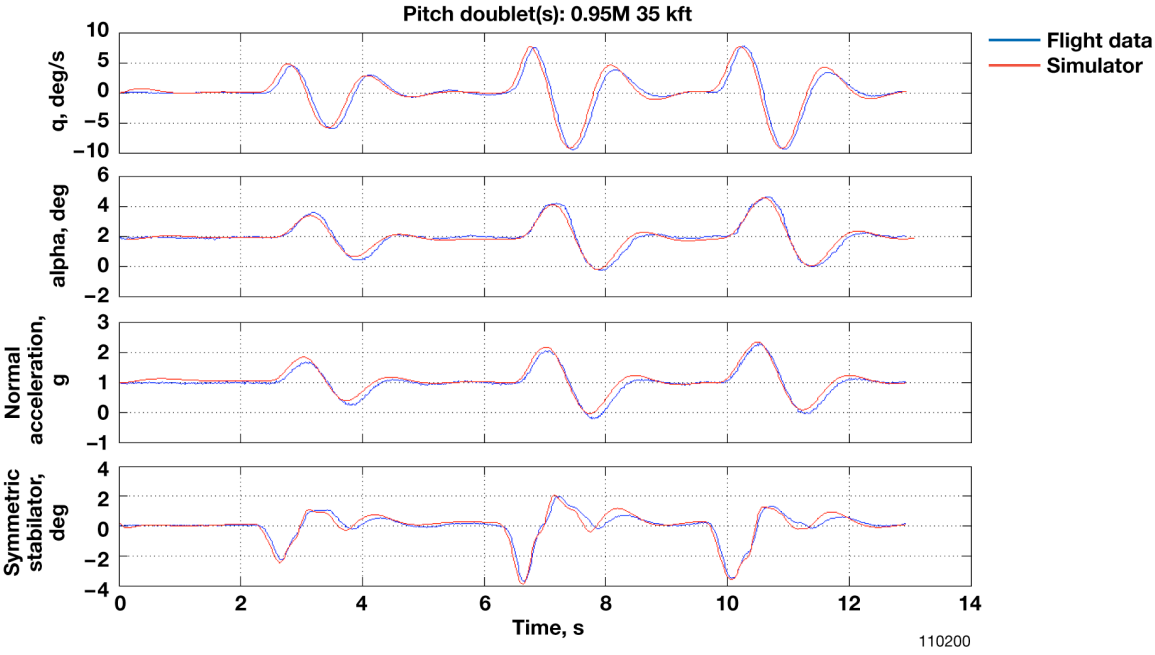

Figure 8. Transonic pitch doublets.

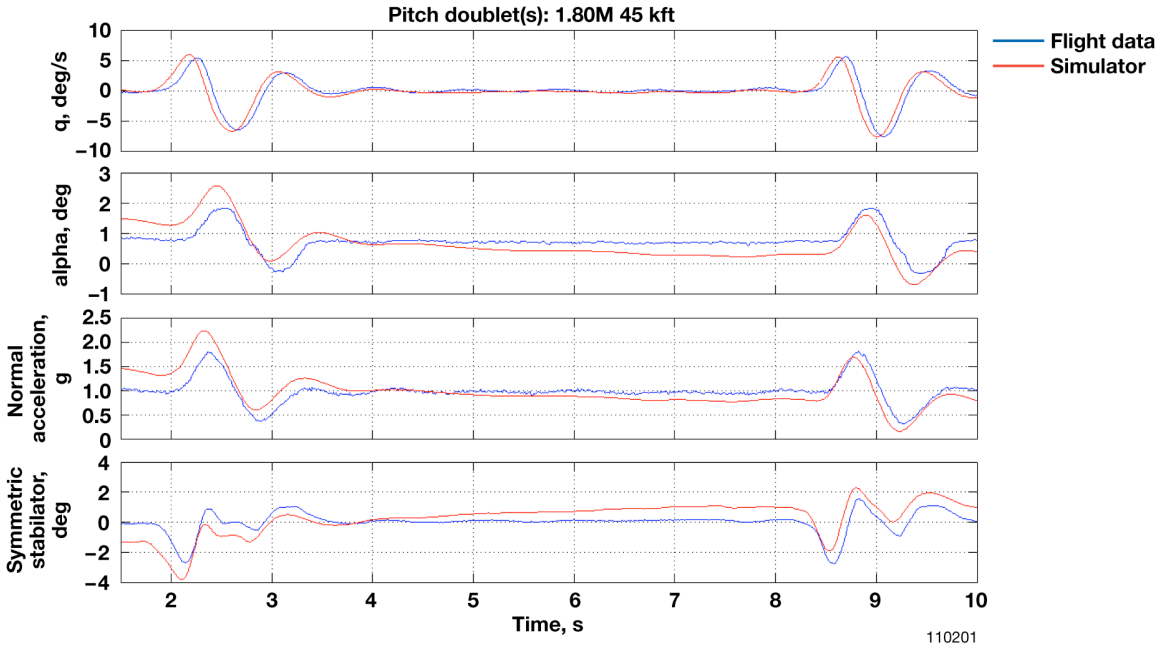

Figure 9. Supersonic pitch doublets.

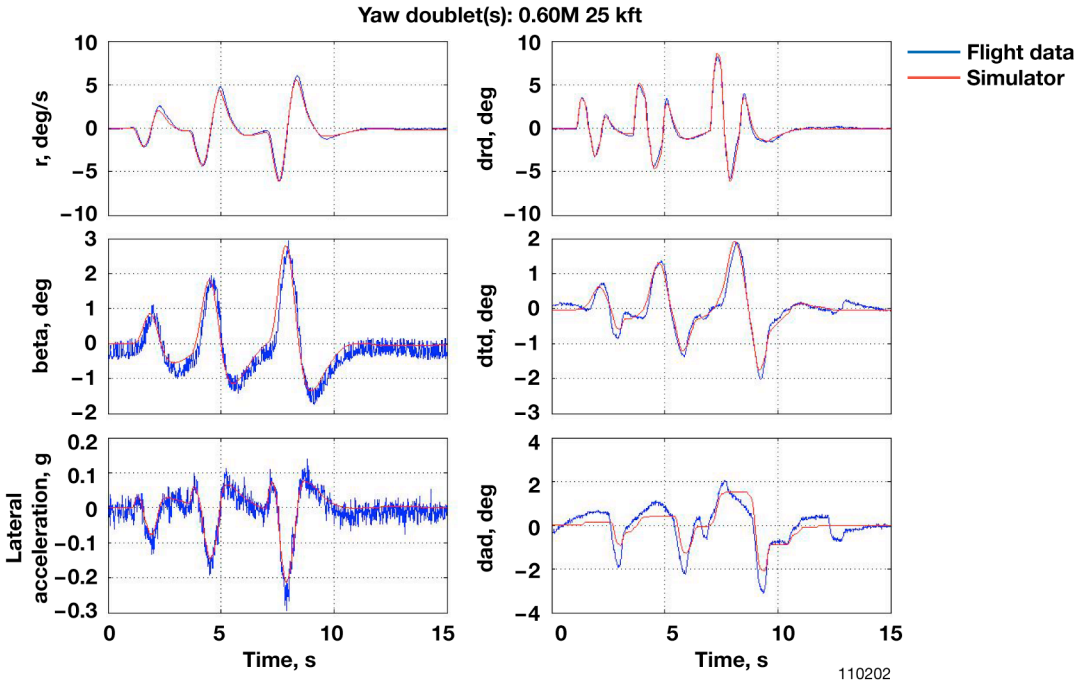

Figure 10. Subsonic yaw doublets.

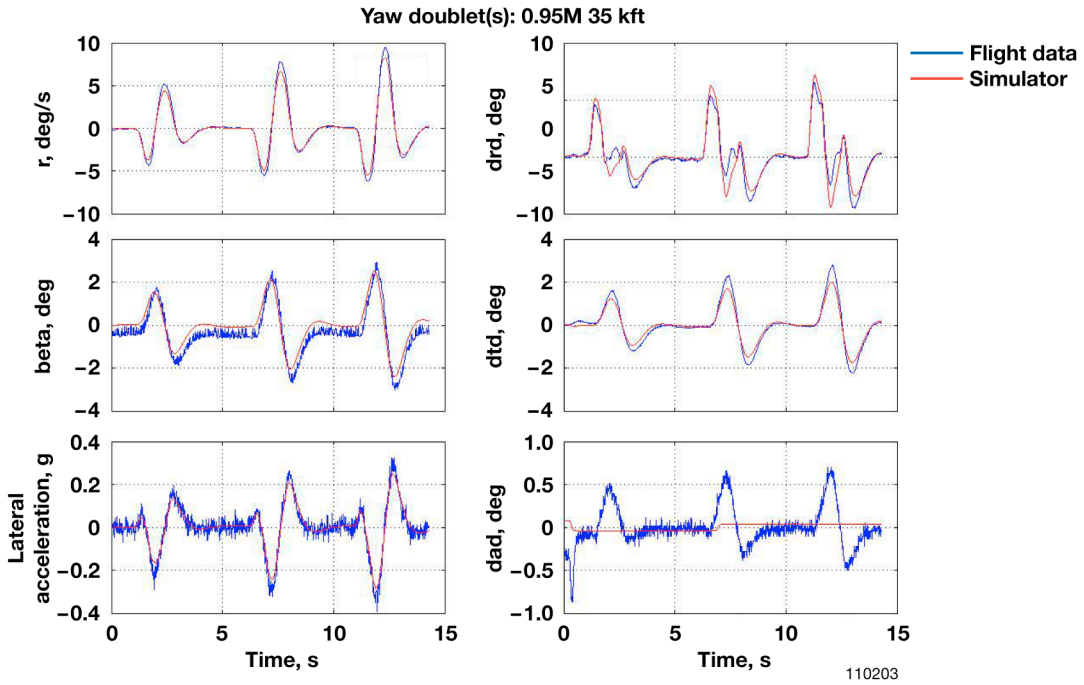

Figure 11. Transonic yaw doublets.

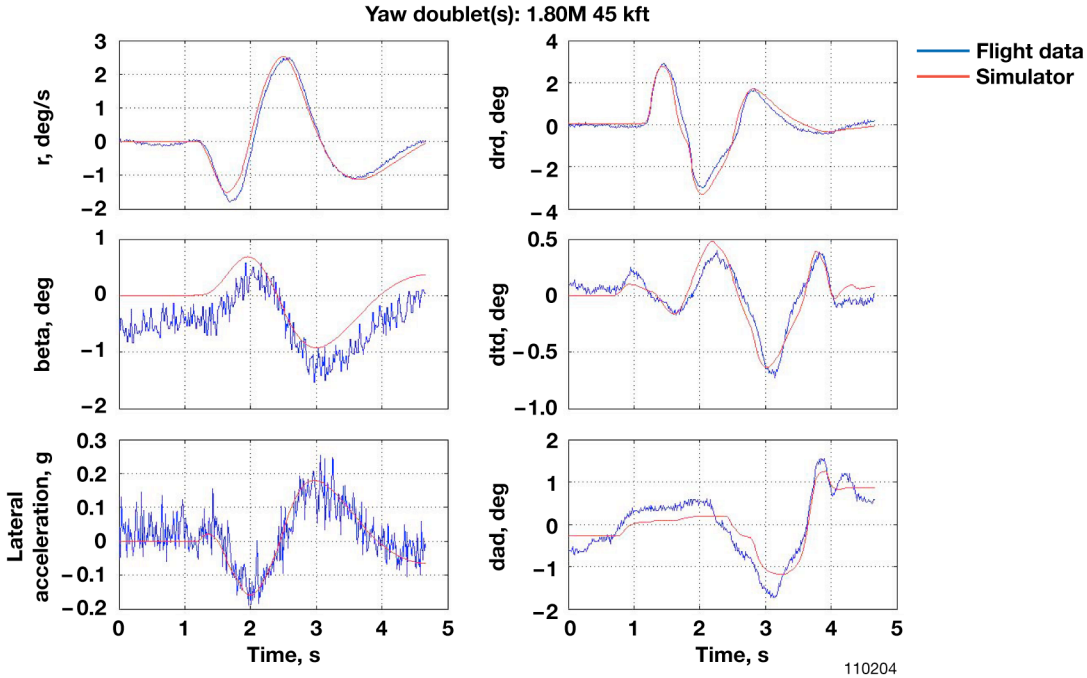

Figure 12. Supersonic yaw doublets.

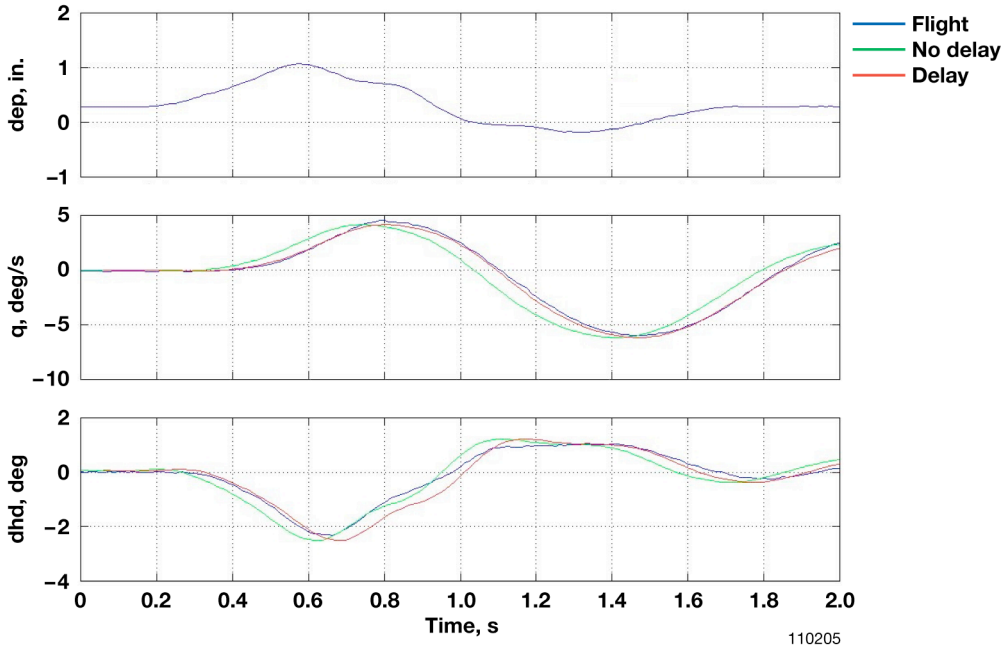

Figure 13. Sixty-millisecond delay in symmetrical stabilator.

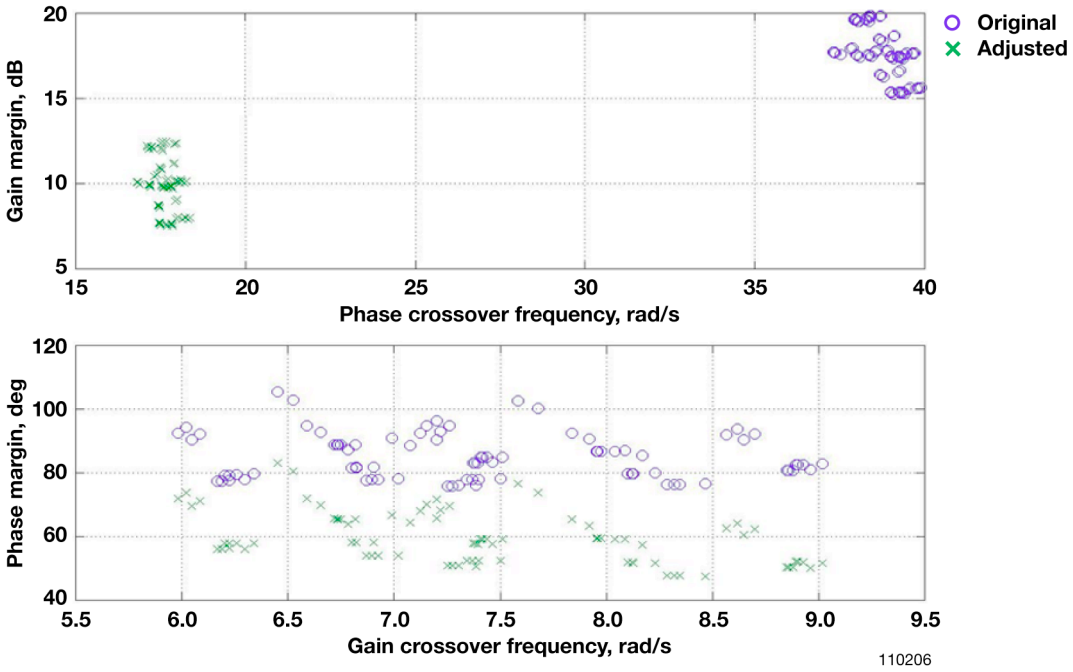

Figure 14. Stability margin reduction due to the 60-ms delay.

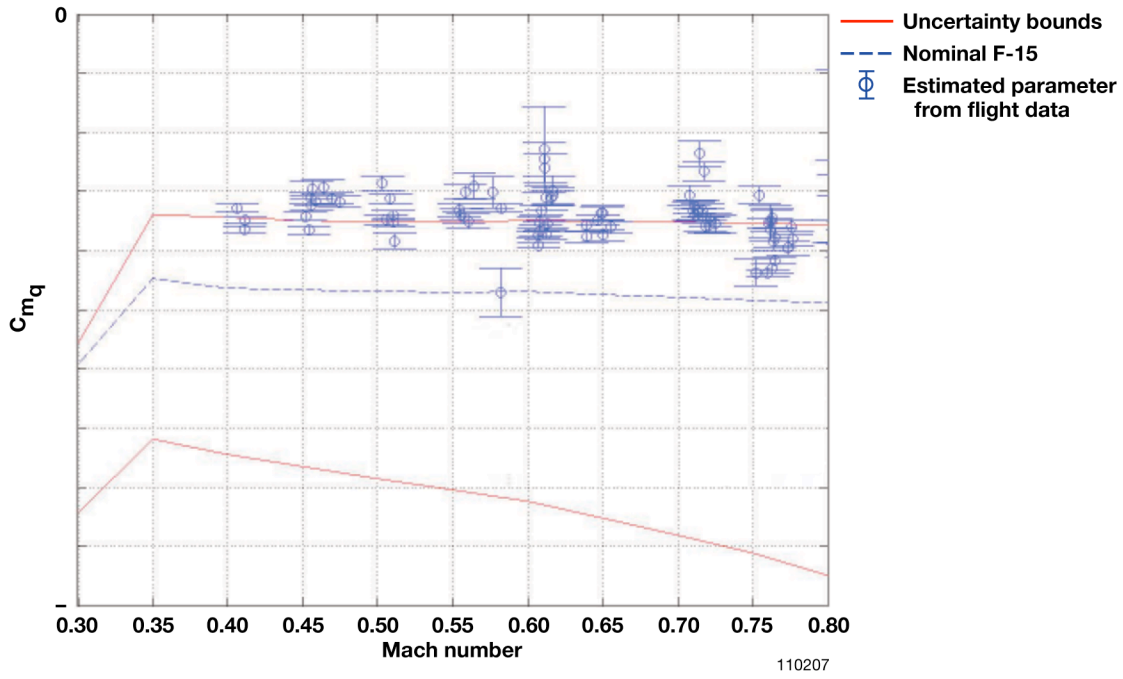

Figure 15. Subsonic derivative border C_{m_q}.

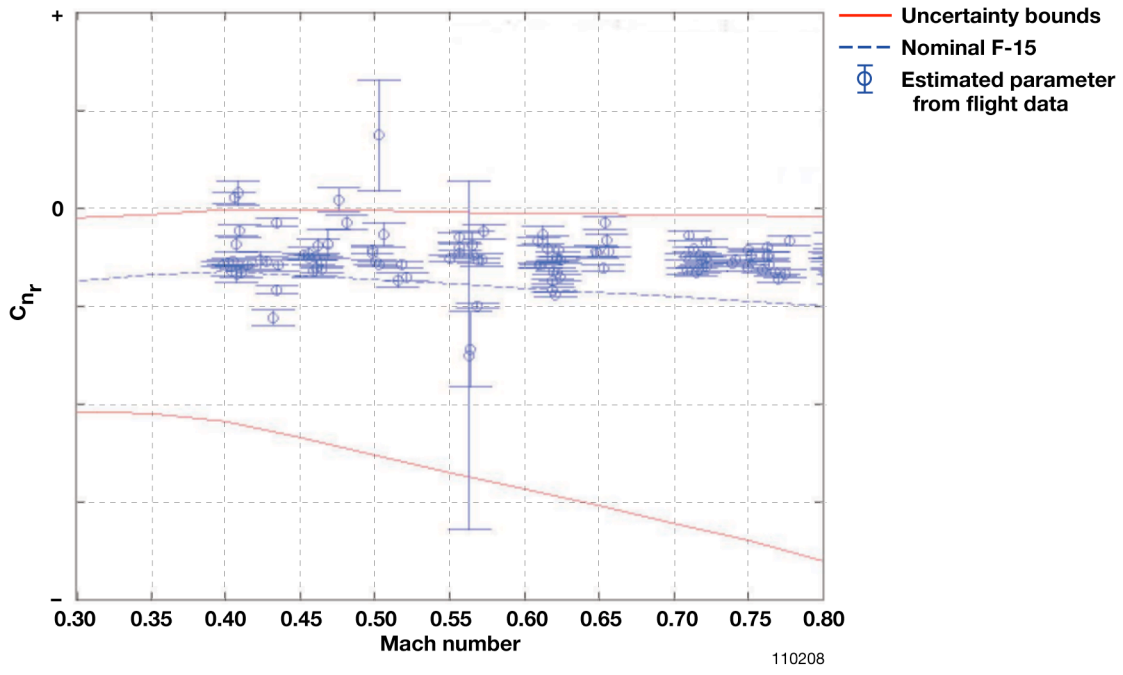

Figure 16. Subsonic derivative border C_{n_r}.

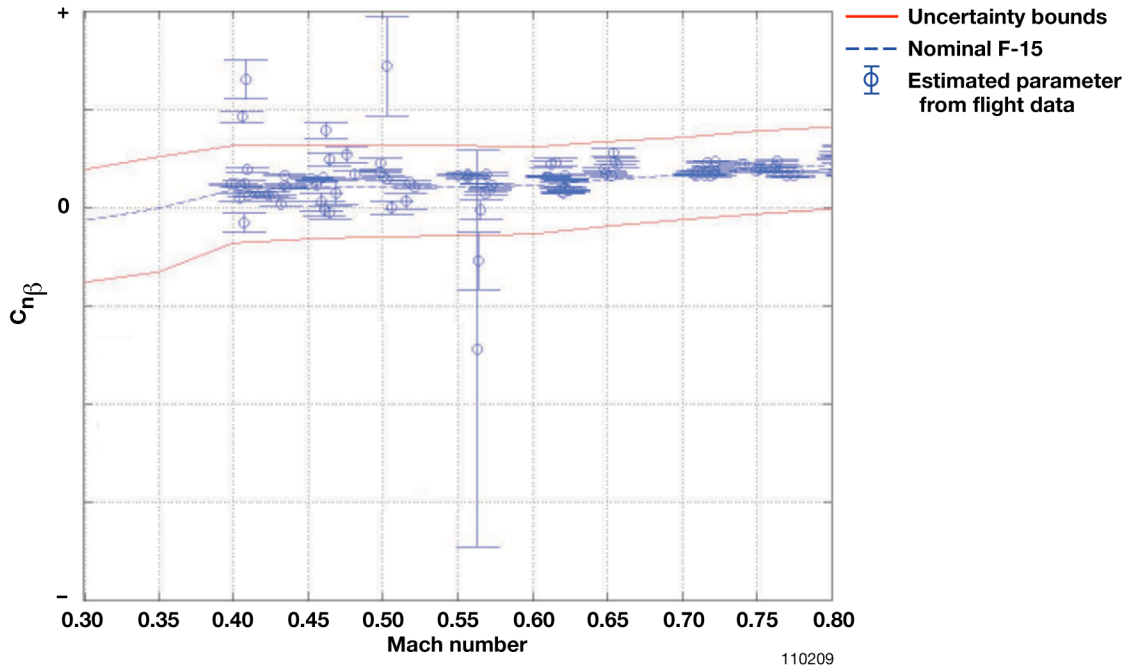

Figure 17. Subsonic derivative border C_{n_β}.

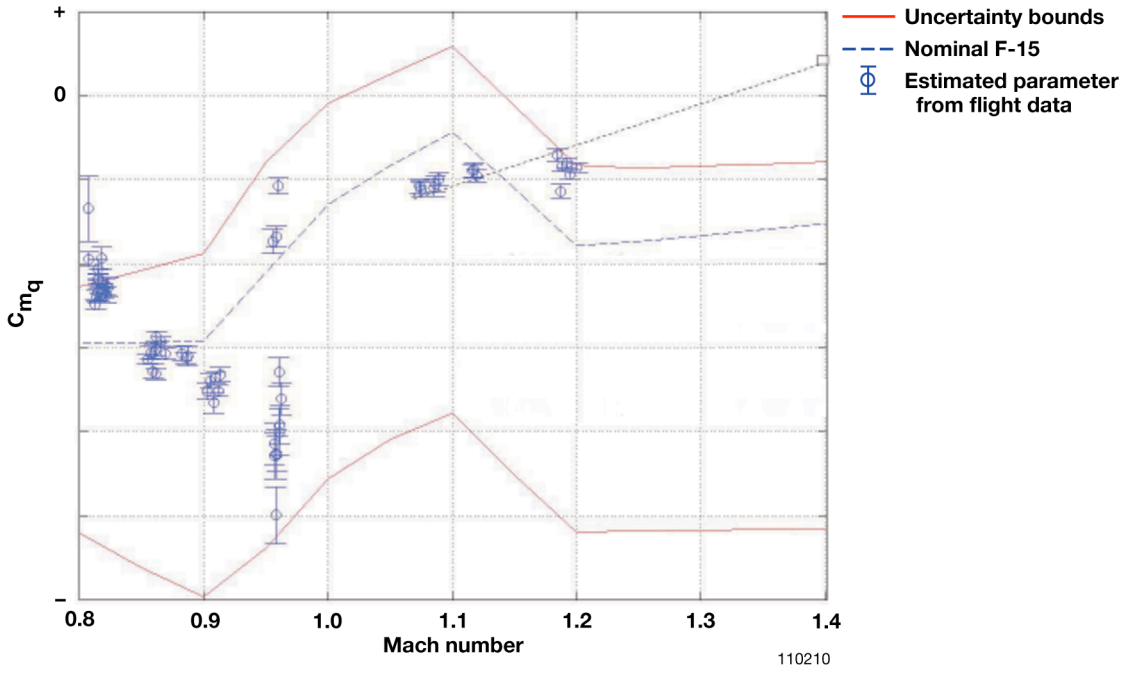

Figure 18. C_{m_q} trend to Mach 1.4.

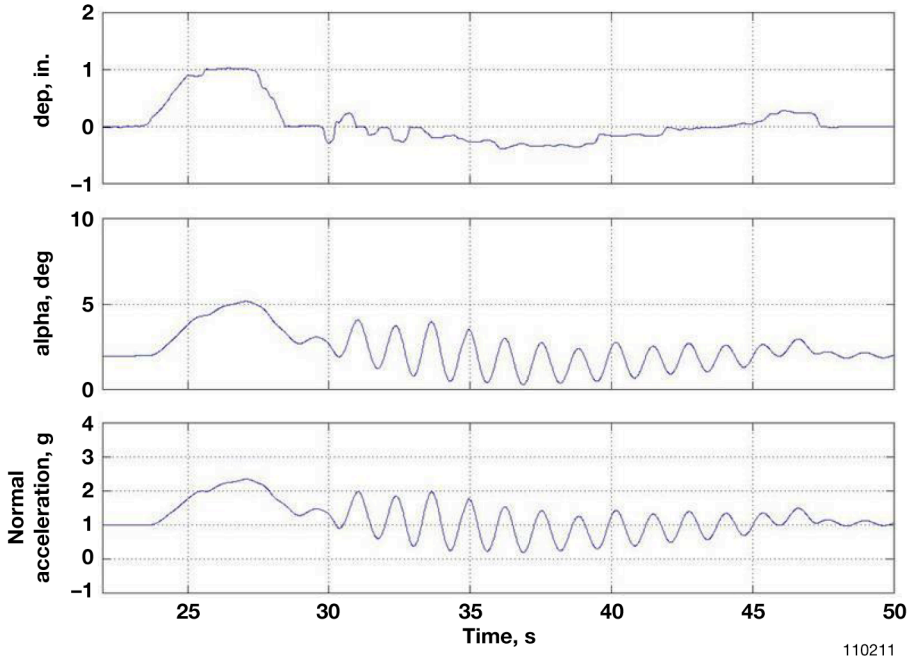

Figure 19. Piloted simulation evaluation at Mach 1.4.

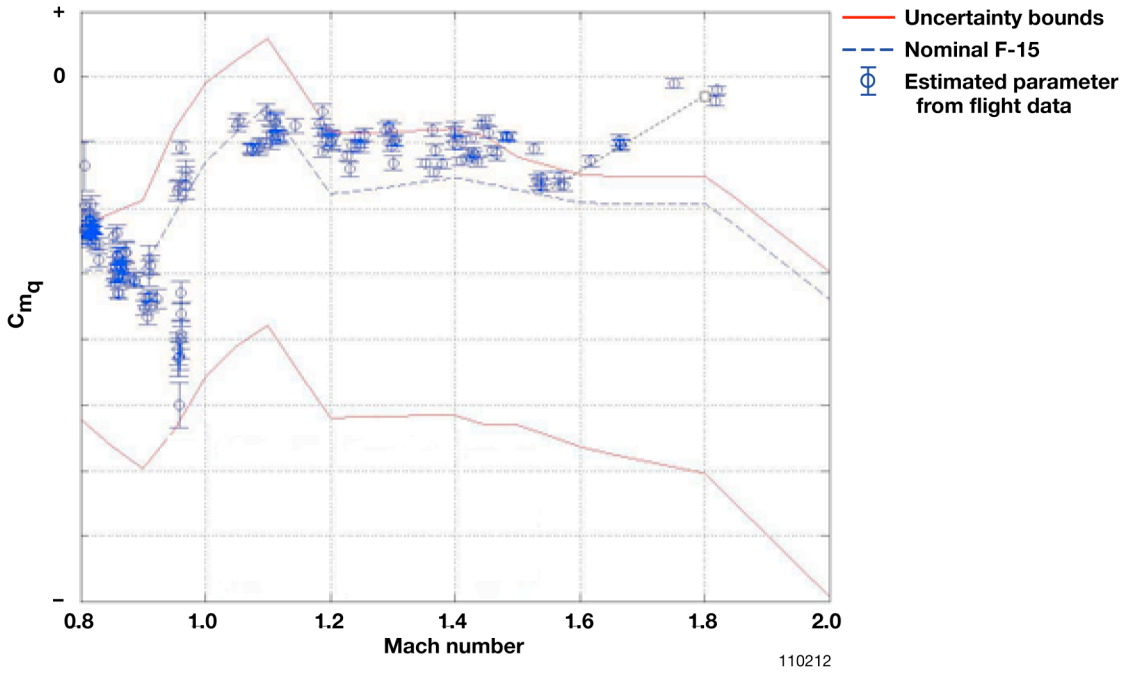

Figure 20. C_{m_q} trend to Mach 1.8.

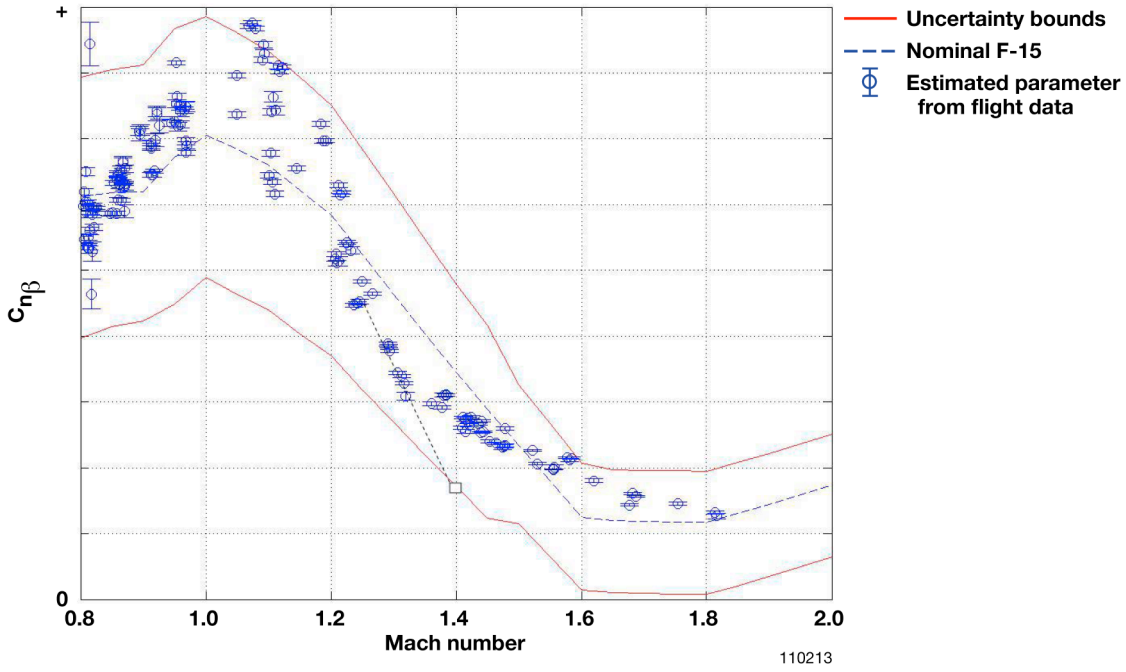

Figure 21. Supersonic derivative border C_{n_β}.

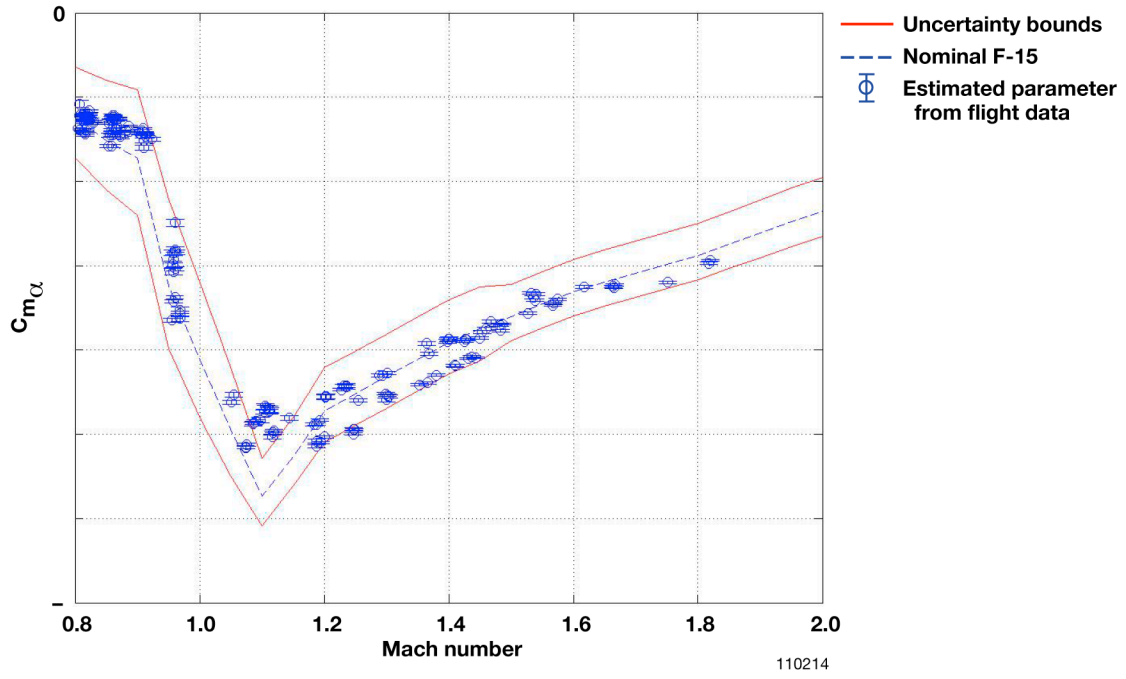

Figure 22. Transonic and supersonic C_{m_α}.

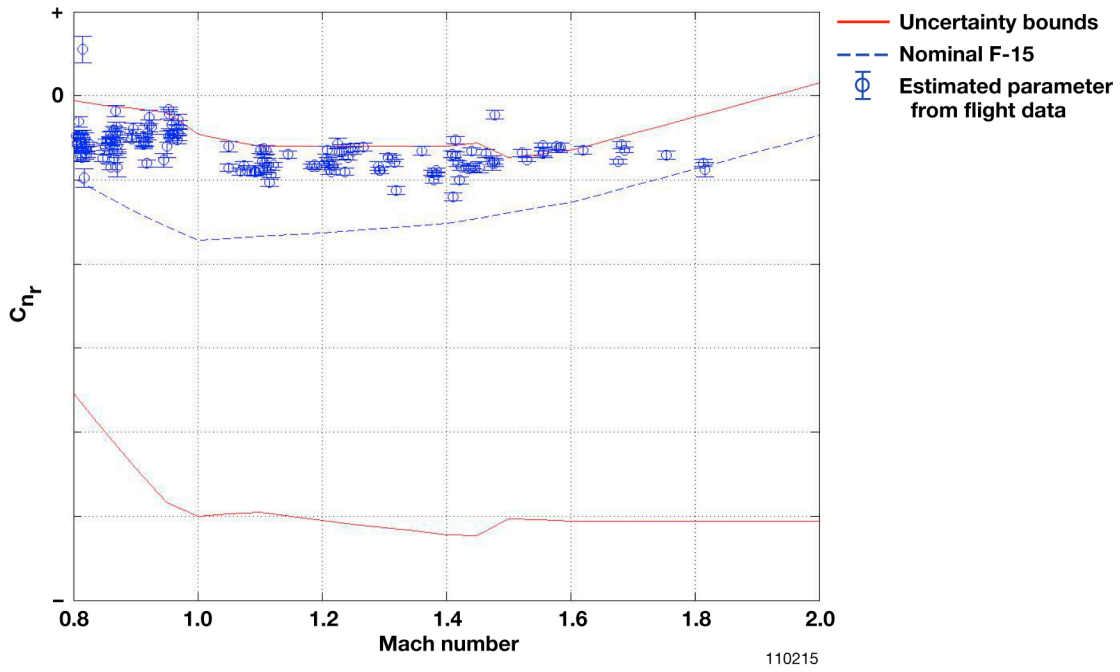

Figure 23. Supersonic derivative border C_{n_r} .

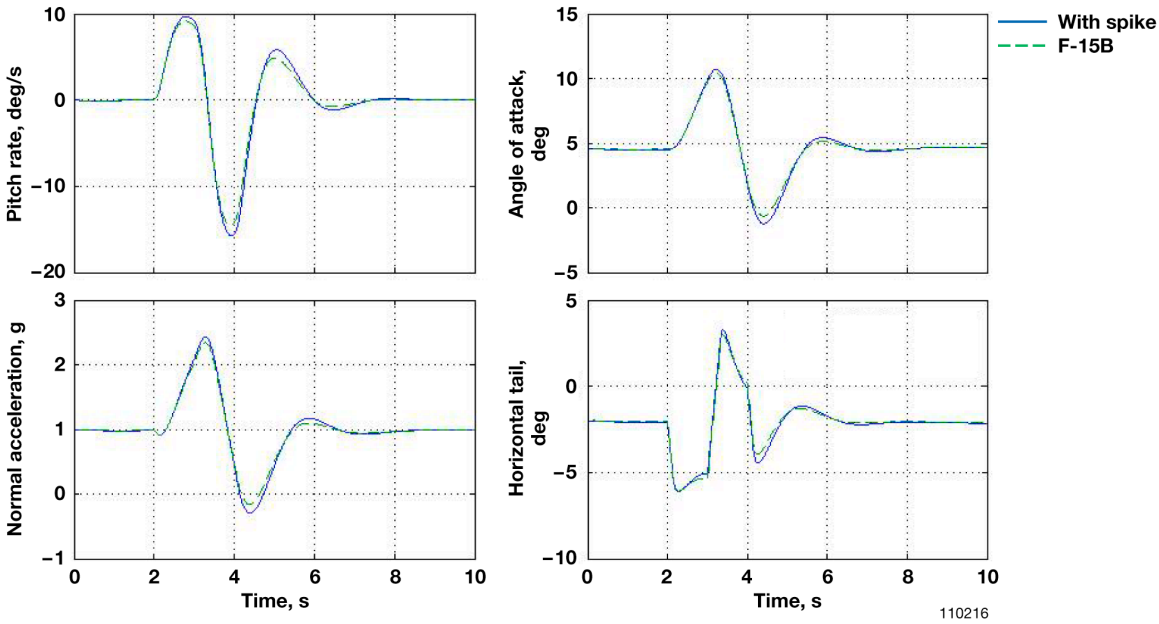

(a) Pitch stick doublet.

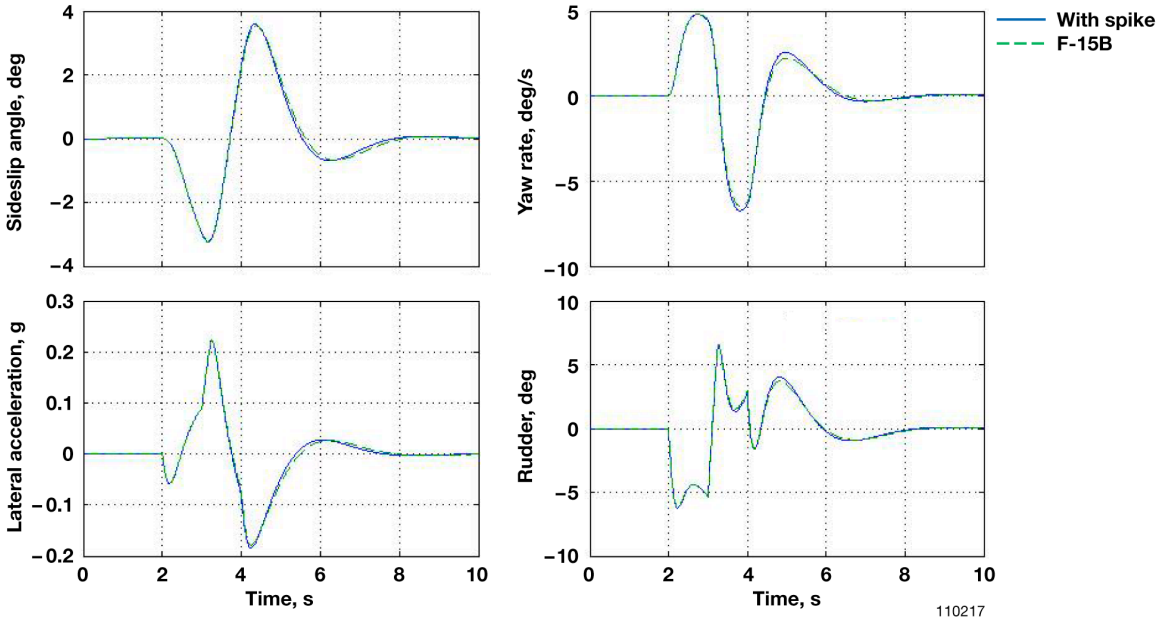

(b) Rudder pedal doublet.

Figure 24. The CAS-“on” simulation comparison of the responses of the test configuration with the baseline F-15B test airplane at flight condition 1.

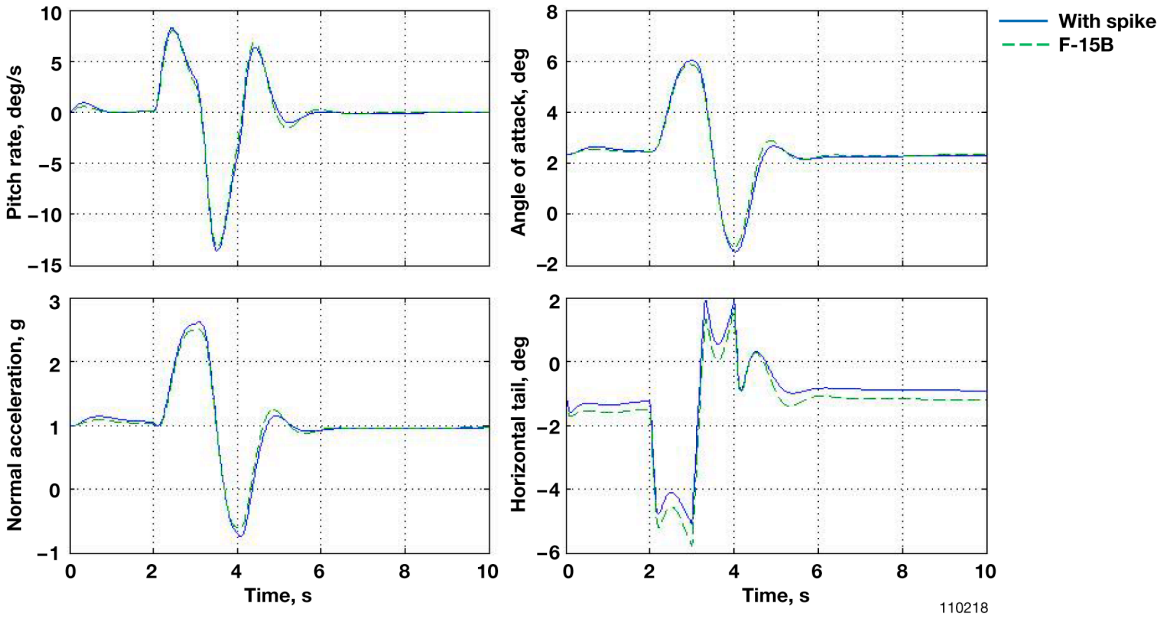

(a) Pitch stick doublet.

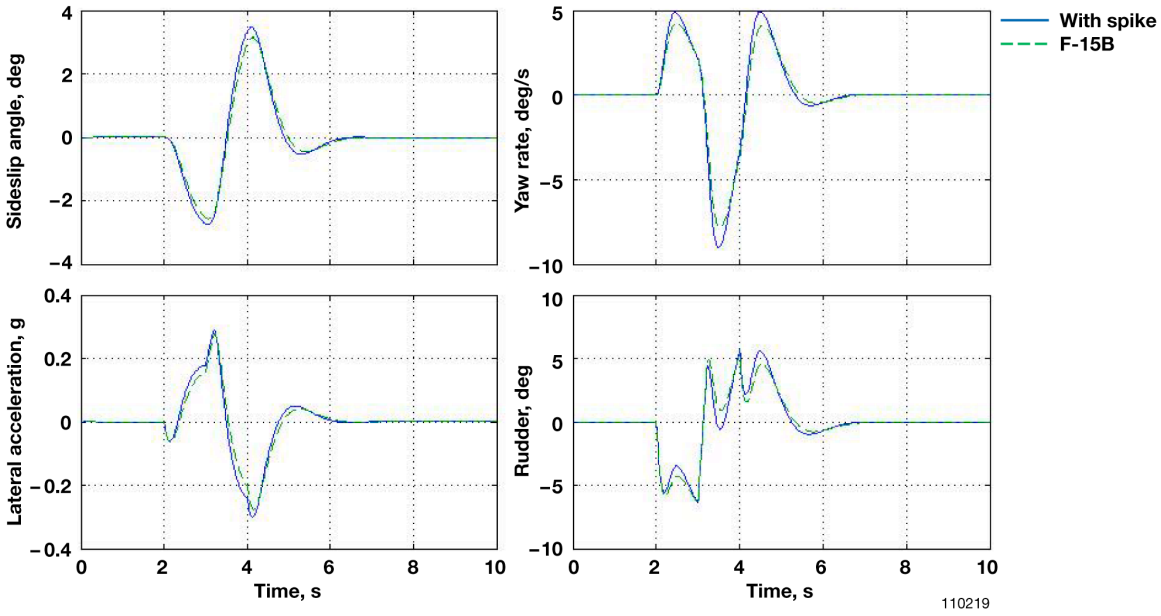

(b) Rudder pedal doublet.

Figure 25. The CAS-“on” simulation comparison of the responses of the test configuration with the baseline F-15B test airplane at flight condition 2.

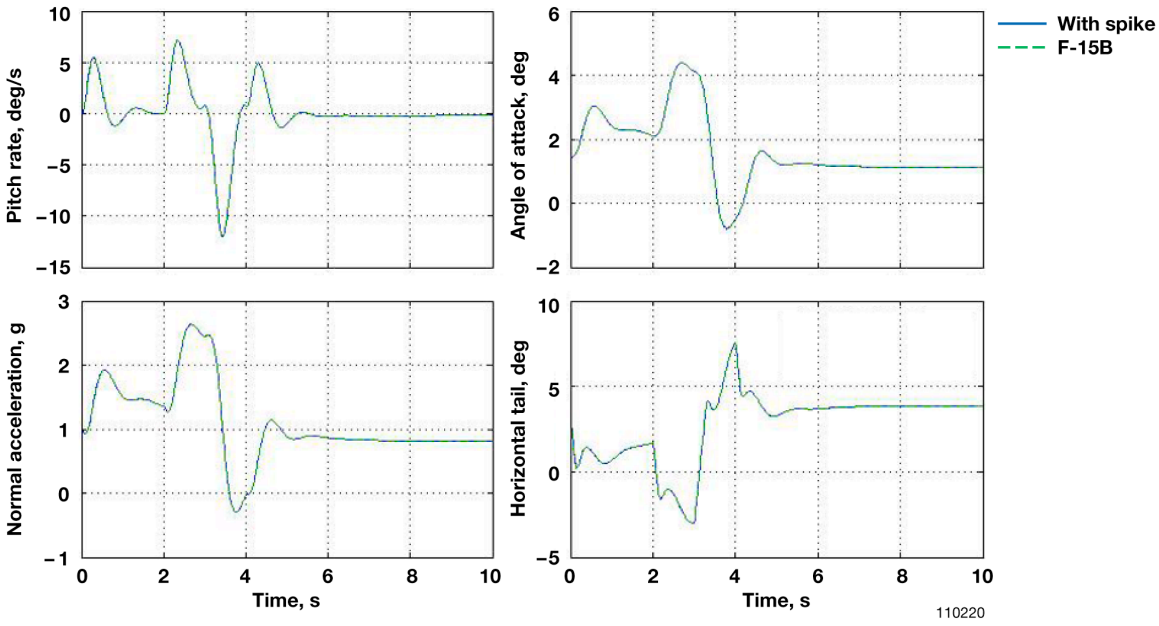

(a) Pitch stick doublet.

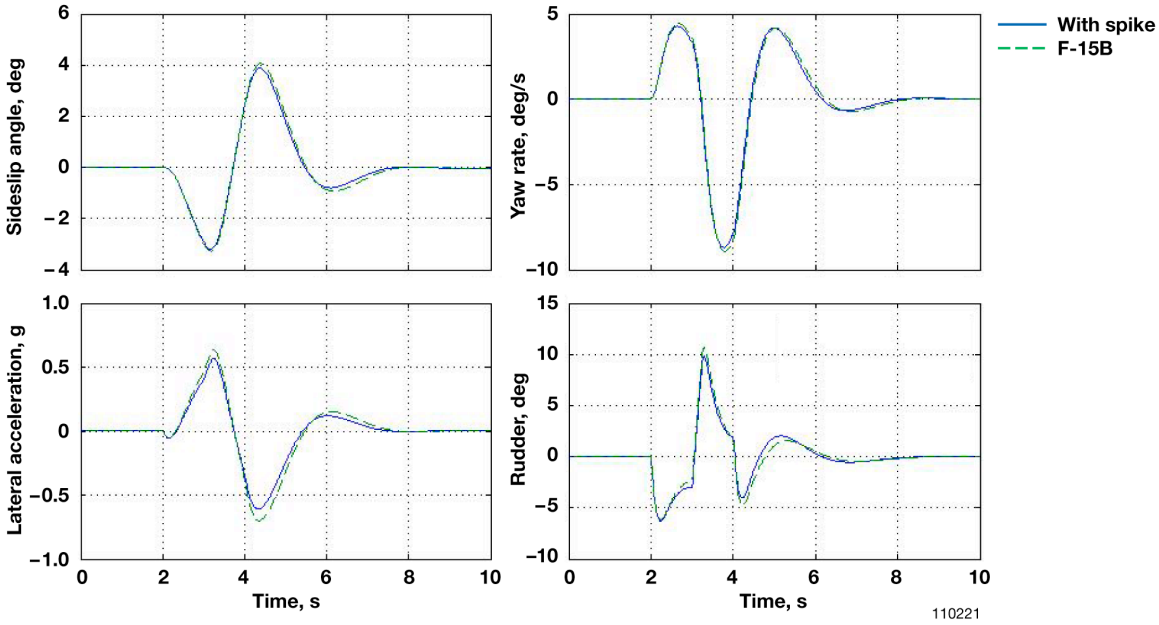

(b) Rudder pedal doublet.

Figure 26. The CAS-"on" simulation comparison of the responses of the test configuration with the baseline F-15B test airplane at flight condition 3.

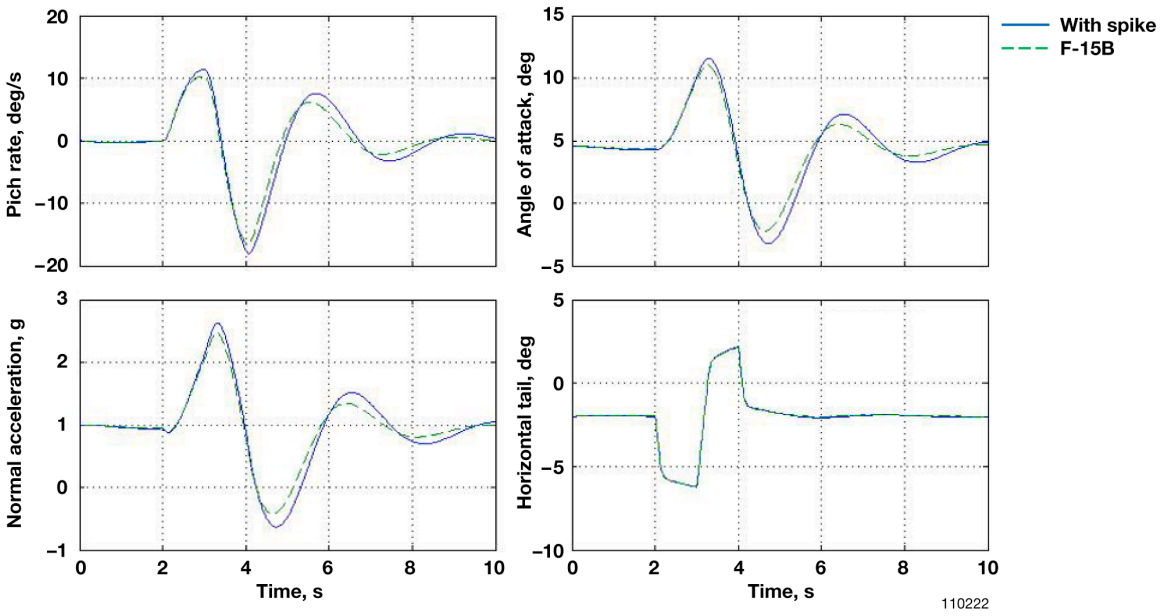

(a) Pitch stick doublet.

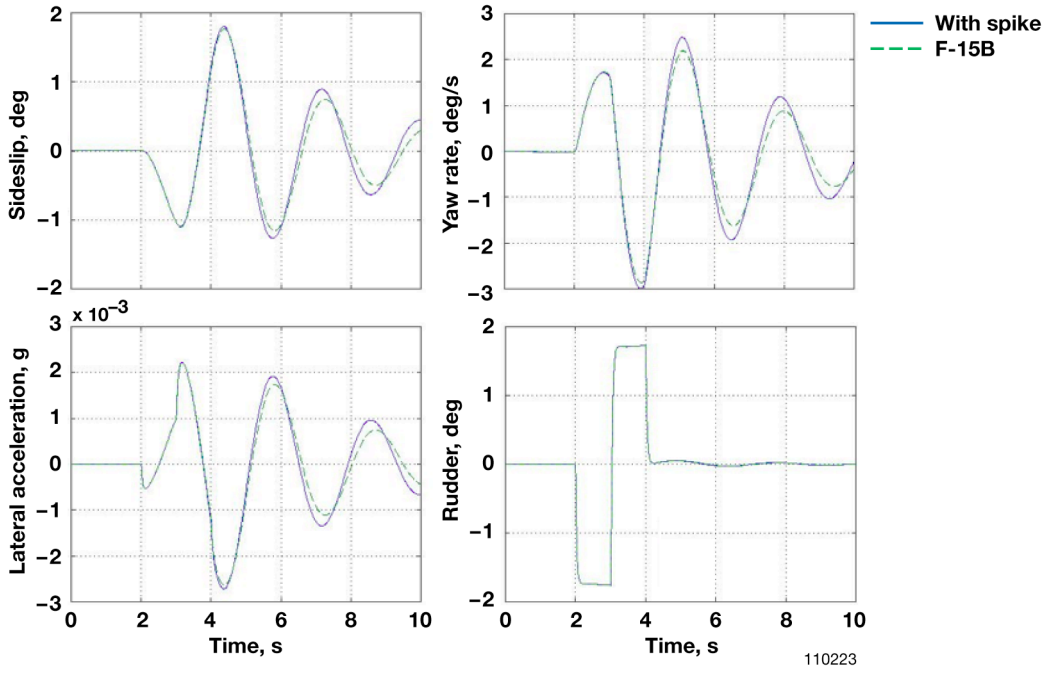

(b) Rudder pedal doublet.

Figure 27. The CAS-“off” comparison of the responses of the test configuration with the baseline F-15B test airplane at flight condition 1.

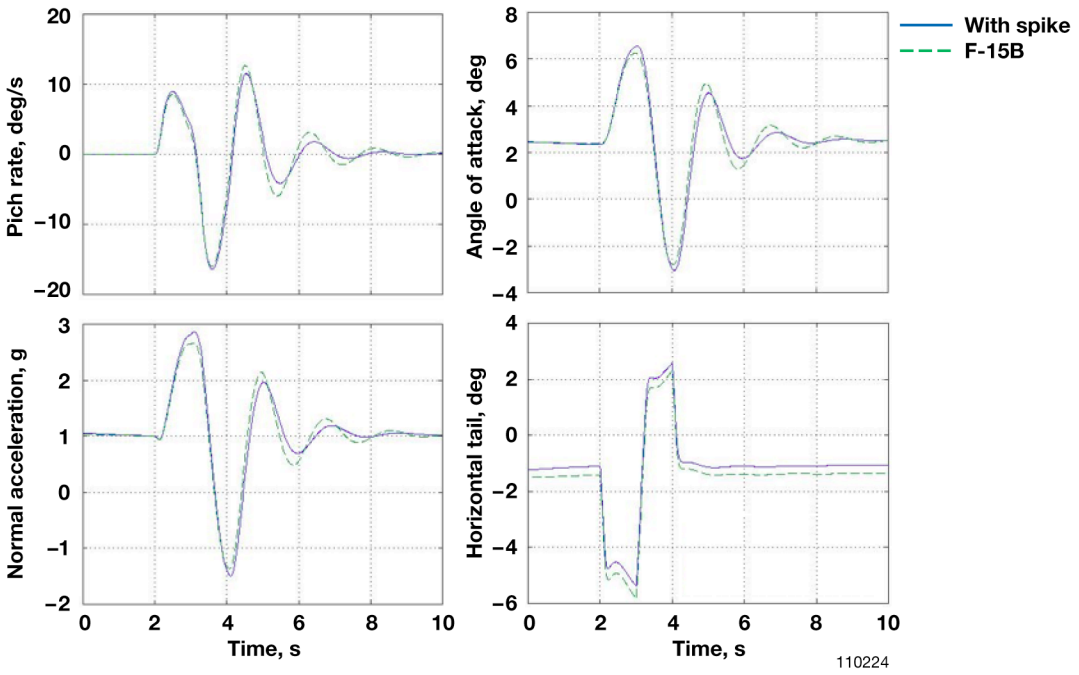

(a) Pitch stick doublet.

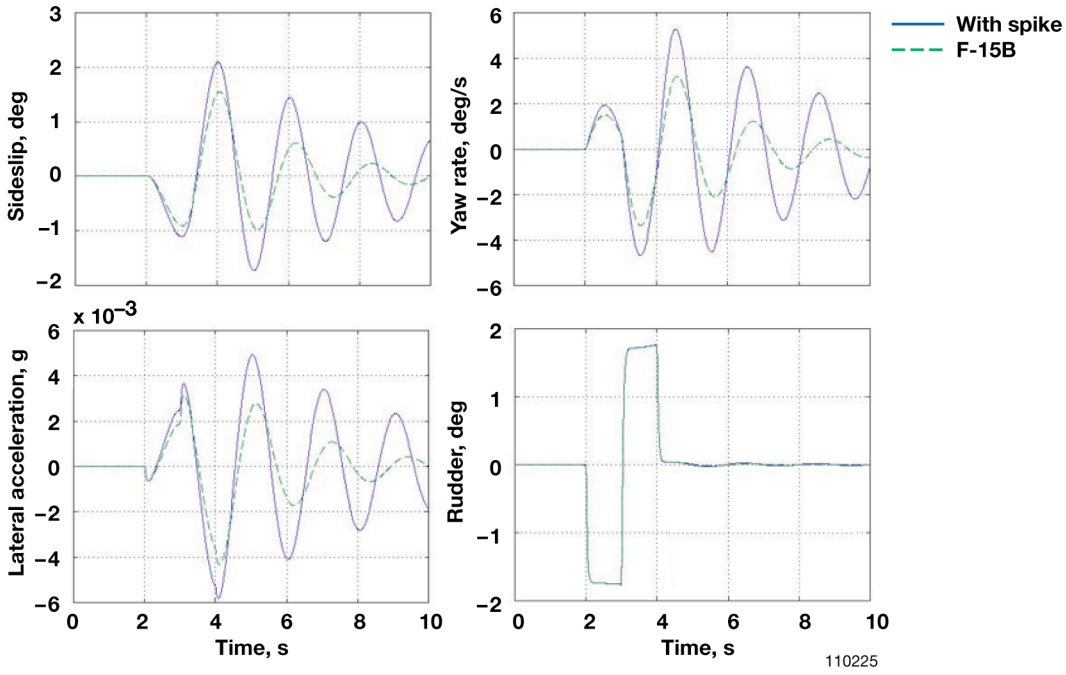

(b) Rudder pedal doublet.

Figure 28. The CAS-"off" comparison of the responses of the test configuration with the baseline F-15B test airplane at flight condition 2.

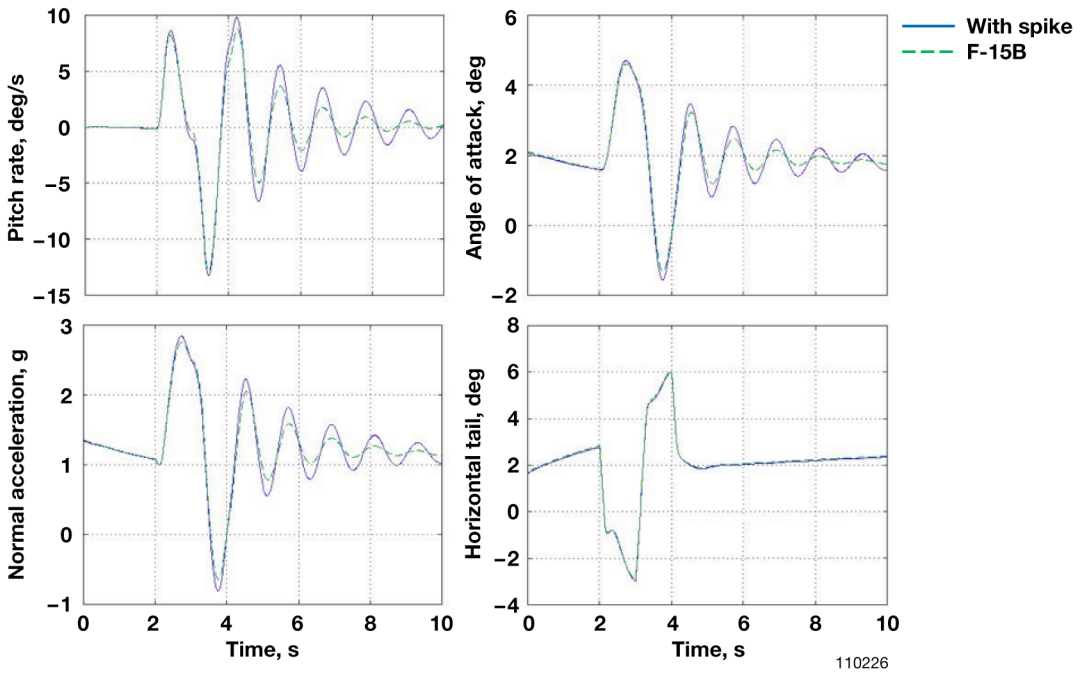

(a) Pitch stick doublet.

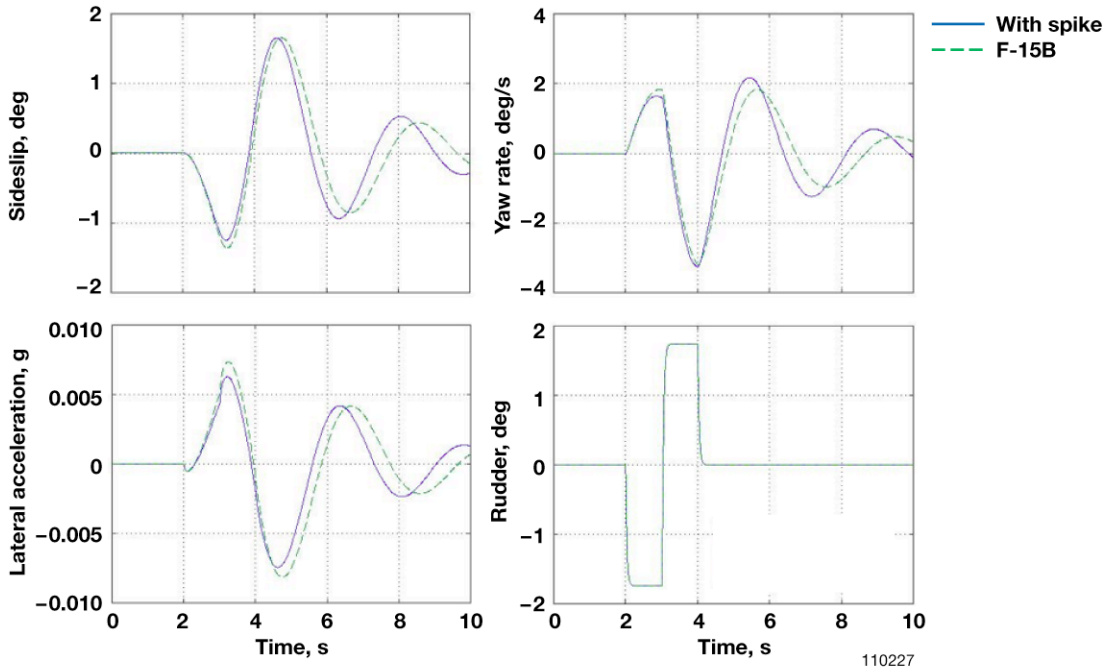

(b) Rudder pedal doublet.

Figure 29. The CAS-"off" comparison of the responses of the test configuration with the baseline F-15B test airplane at flight condition 3.

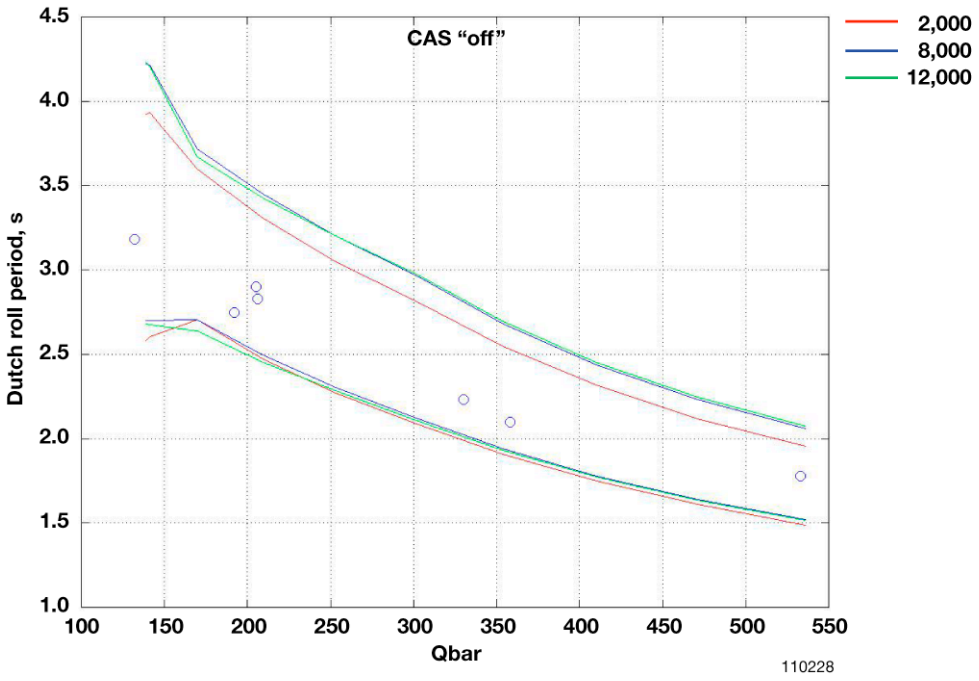

Figure 30. Subsonic CAS-"off" Dutch roll period.

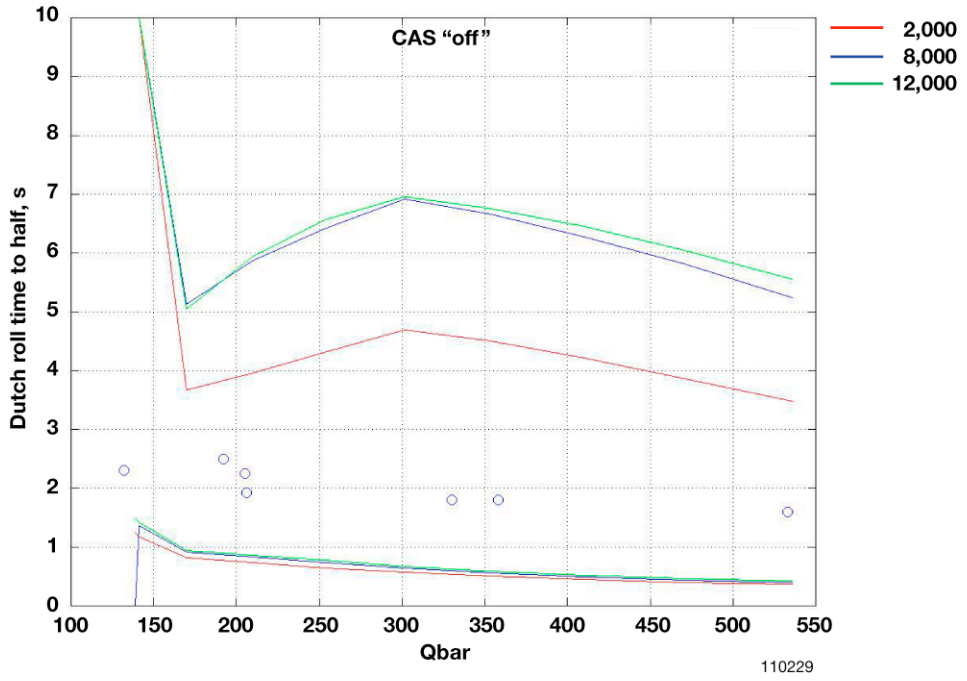

Figure 31. Subsonic CAS-"off" Dutch roll time to half.

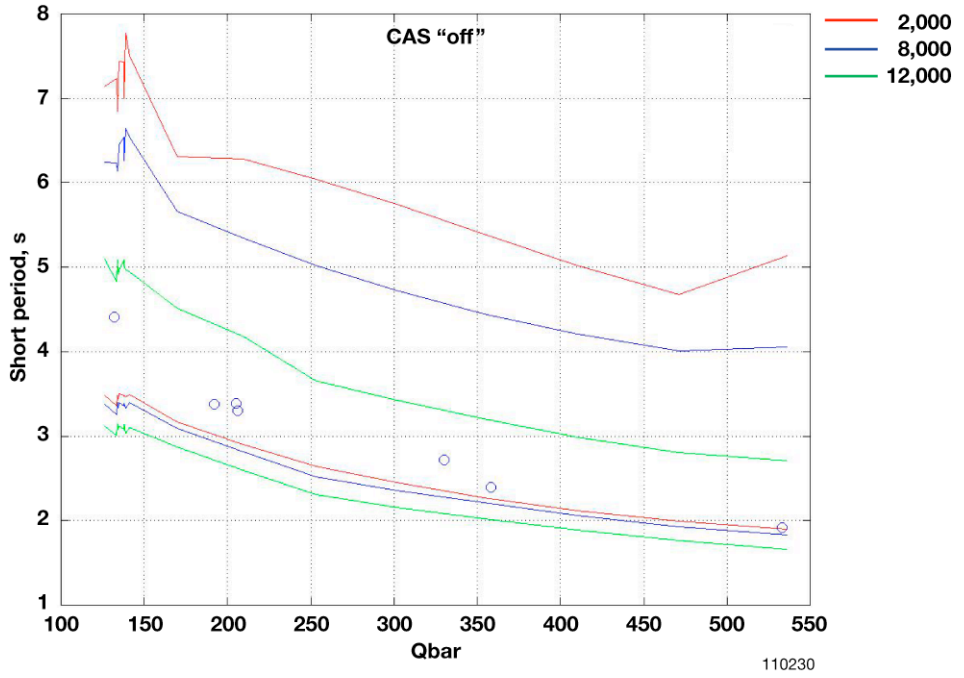

Figure 32. Subsonic CAS-"off" short period.

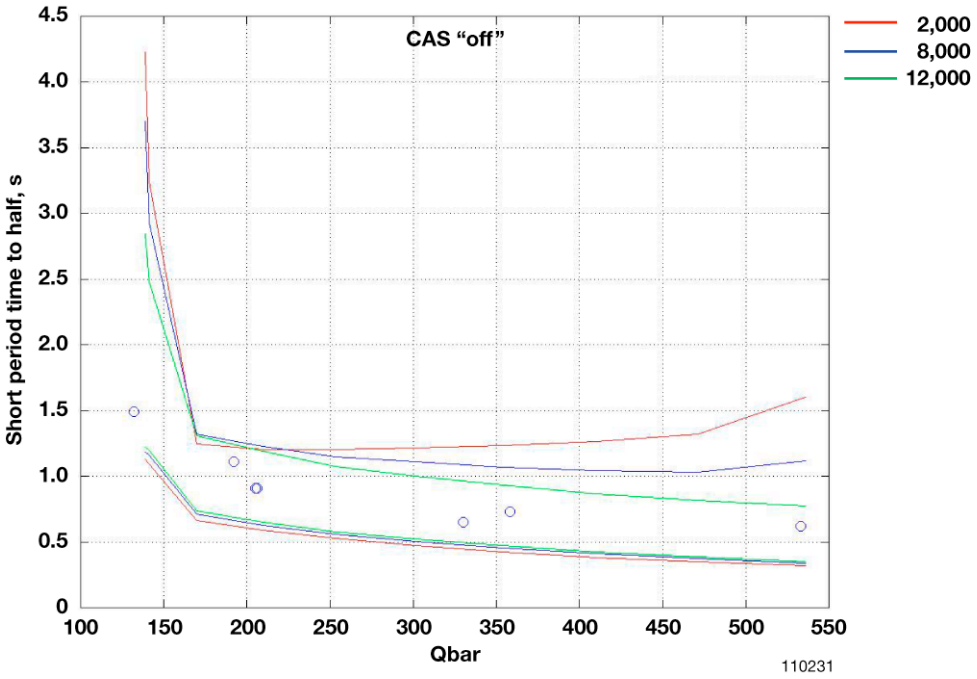

Figure 33. Subsonic CAS-"off" Dutch roll time to half.

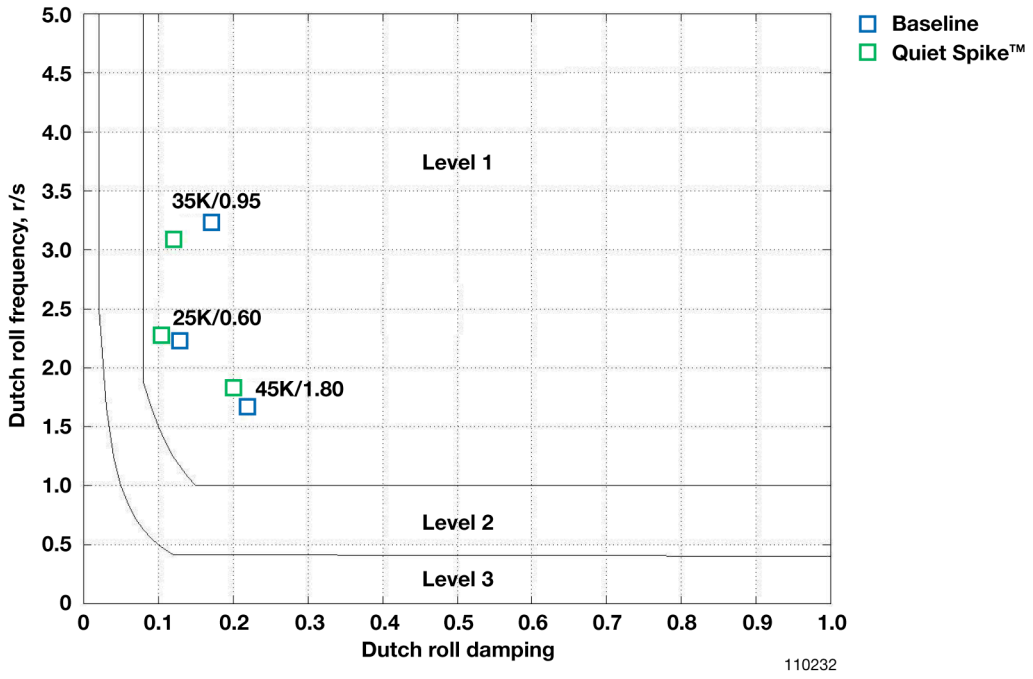

Figure 34. The CAS-"off" yaw axis handling qualities evaluation of flight conditions 1, 2, and 3.

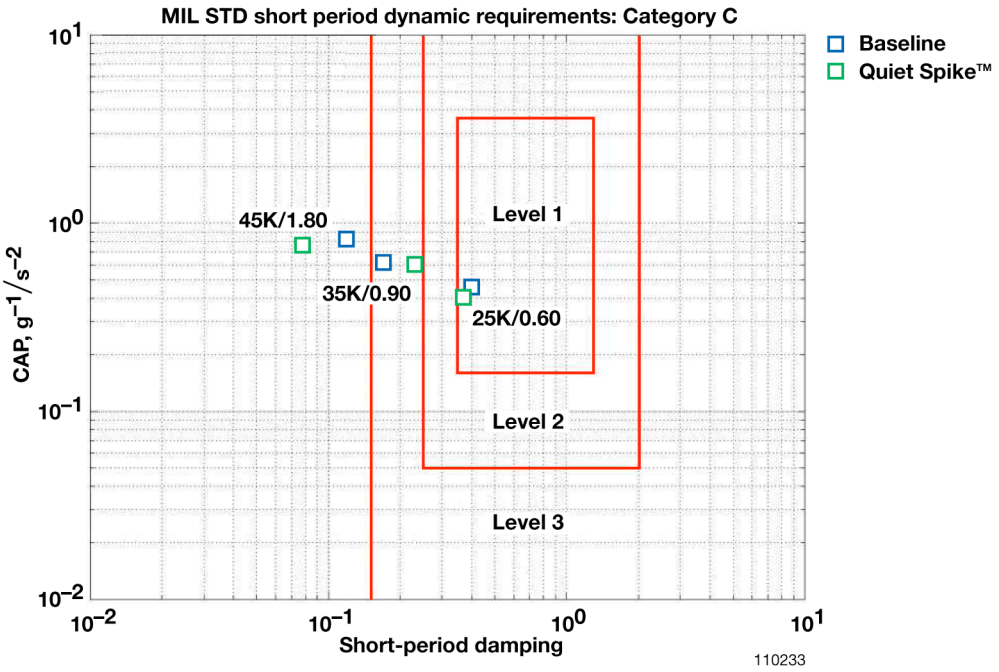

Figure 35. The CAS-"off" pitch axis handling qualities evaluation of a subsonic, a transonic, and a supersonic flight condition.

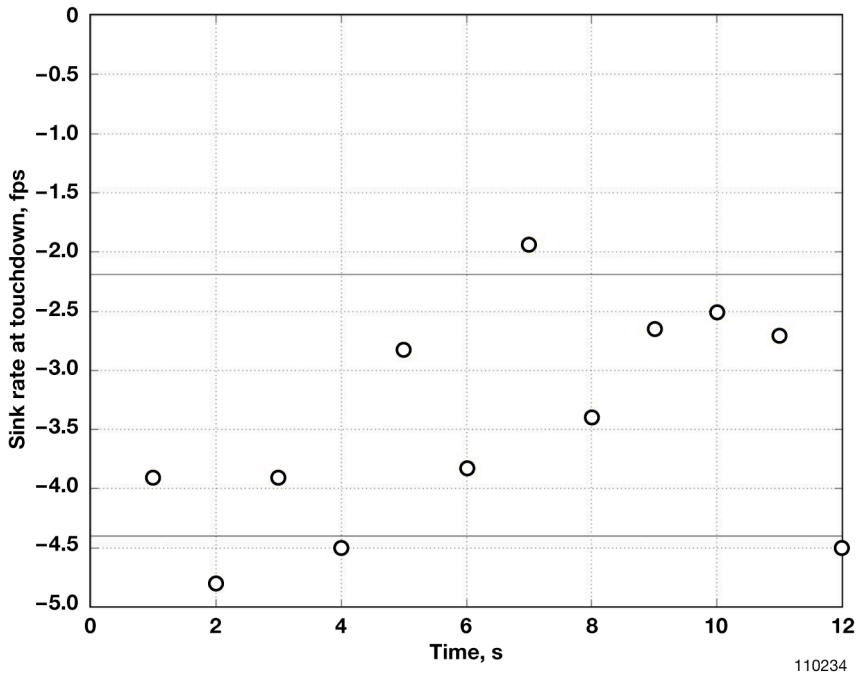

Figure 36. The estimated sink rate at touchdown compared to a targeted range.

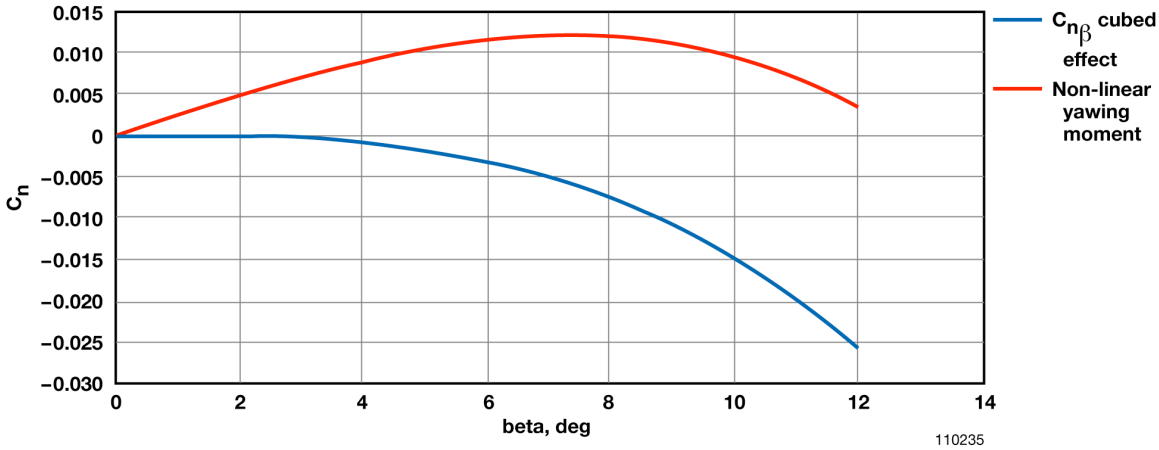

Figure 37. The non-linear yawing moment contribution to the simulation.

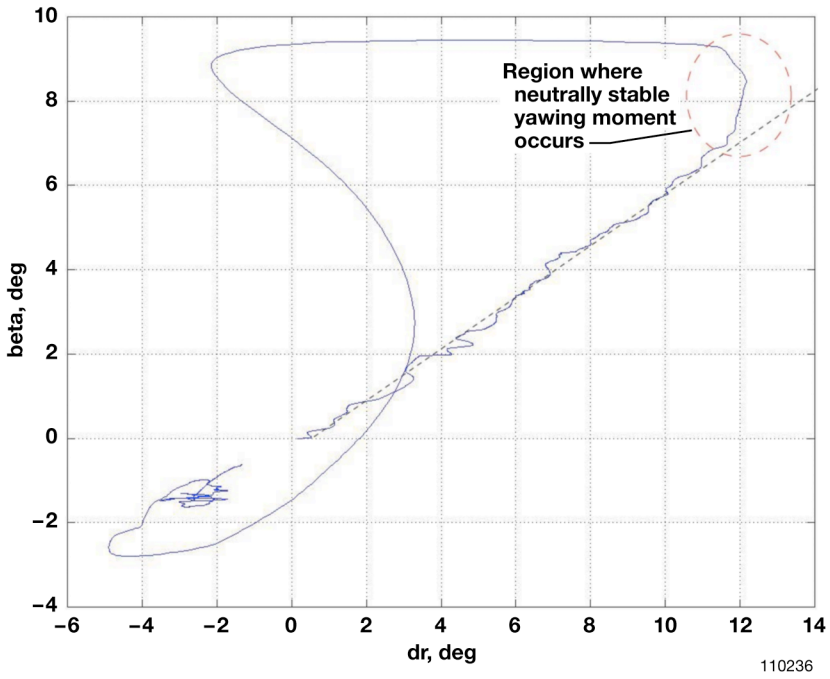

Figure 38. Simulation cross plot of sideslip and rudder during a wings-level sideslip sweep.

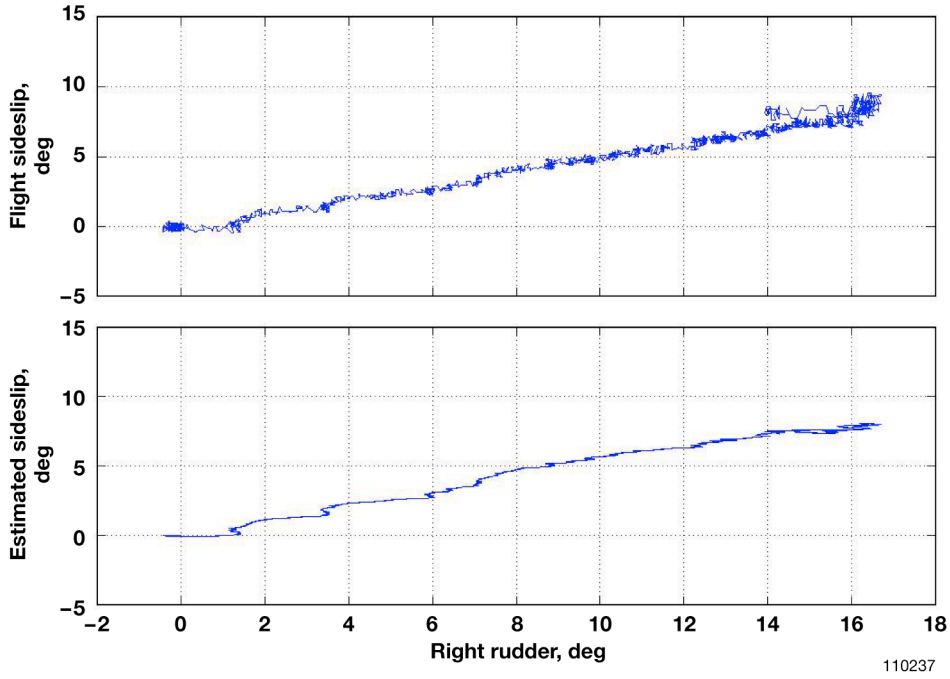

Figure 39. Elevated beta versus rudder cross plot.

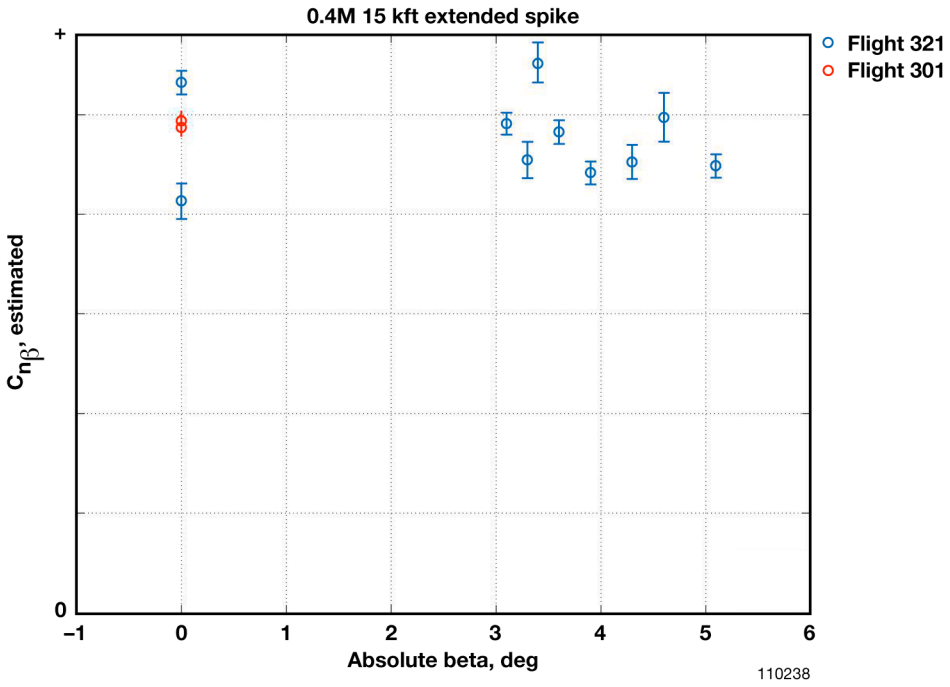

Figure 40. C_{n_β} versus beta.

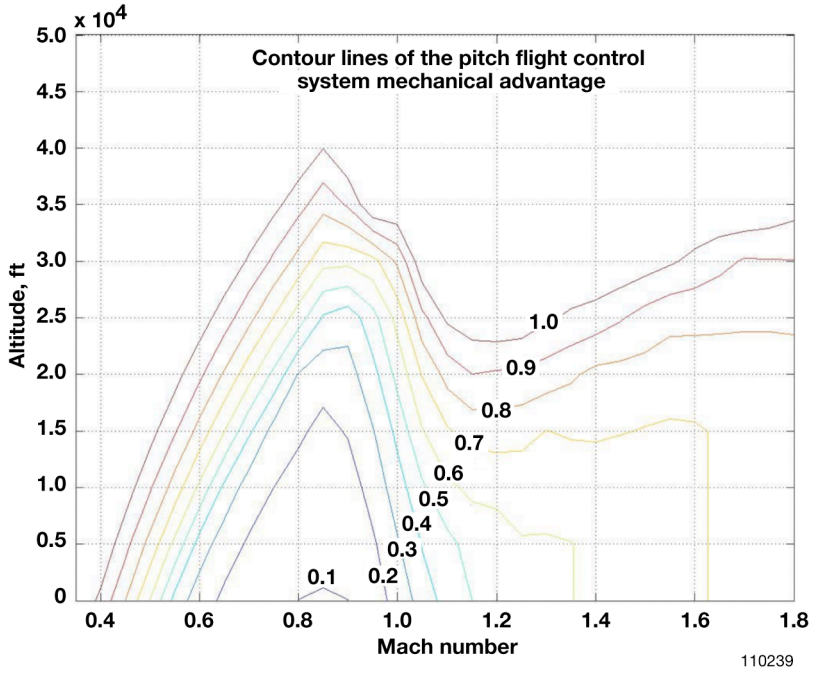

Figure 41. Contour plot of pitch ratio gauge with flight condition.

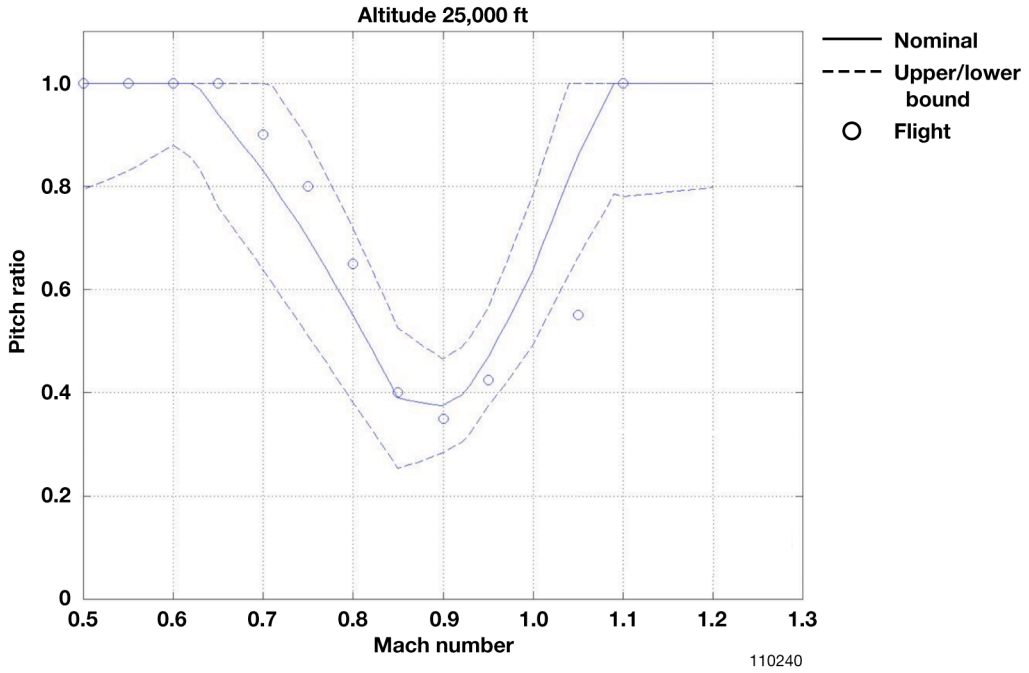

Figure 42. Pitch ratio gauge versus Mach number at an altitude of 25,000 ft.